Breakup of a fluid thread in a confined geometry: droplet-plug transition, perturbation sensitivity, and kinetic stabilization with confinement

John G. Hagedorn,[1] Nicos S. Martys,[2] and Jack F. Douglas[3]
[1]*Mathematical and Computational Sciences Division, NIST, Gaithersburg, Maryland 20899, USA*
[2]*Materials and Construction Research Division, NIST, Gaithersburg, Maryland 20899, USA*
[3]*Polymers Division, NIST, Gaithersburg, Maryland 20899, USA*
(Received 3 March 2003; published 27 May 2004)

We investigate the influence of geometrical confinement on the breakup of long fluid threads in the absence of imposed flow using a lattice Boltzmann model. Our simulations primarily focus on the case of threads centered coaxially in a tube filled with another Newtonian fluid and subjected to both impulsive and random perturbations. We observe a significant slowing down of the rate of thread breakup ("kinetic stabilization") over a wide range of the confinement, $\Lambda = R_{\mathrm{tube}}/R_{\mathrm{thread}} \leqslant 10$ and find that the relative surface energies of the liquid components influence this effect. For $\Lambda < 2.3$, there is a transition in the late-stage morphology between spherical droplets and tube "plugs." Unstable distorted droplets ("capsules") form as transient structures for intermediate confinement ($\Lambda \approx 2.1-2.5$). Surprisingly, the thread breakup process for more confined threads ($\Lambda \leqslant 1.9$) is found to be sensitive to the nature of the intial thread perturbation. Localized impulsive perturbations ("taps") cause a "bulging" of the fluid at the wall, followed by thread breakup through the propagation of a wavelike disturbance ("end-pinch instability") initiating from the thread rupture point. Random impulses along the thread, modeling thermal fluctuations, lead to a complex breakup process involving a competition between the Raleigh and end-pinch instabilities. We also briefly compare our tube simulations to threads confined between parallel plates and to multiple interacting threads under confinement.

DOI: 10.1103/PhysRevE.69.056312 PACS number(s): 47.20.Dr, 47.11.+j, 47.20.Hw

I. INTRODUCTION

The breakup of fluid threads and films by capillary instability is ubiquitous in engineering, science, and nature. For example, an understanding of this phenomenon is essential to the the technologies of ink-jet printing [1], the production of stable thin coatings (e.g., polymer films, coating optical fibers, and wires) [2], the morphology and stability of extruded polymer blends [3,4], the formation of polymer fibers from polymer blends [5], the transportation of oil in pipelines [6–9], and tertiary oil recovery [10(a)]. In many of these technological applications, thread breakup occurs under tubular confinement conditions. Examples include the phase separation of blends and other fluid mixtures in porous media or in the presence of large quantities of filter particles where a near tubular geometry exists locally, oil recovery from porous rocks [10(a)] and synthetic tubular networks encountered in multicomponent fluid processing, ranging in scale from plant pipelines to microfluidic devices [6–9,10(b)]. Moreover, the consequences of this type of instability are apparent in a multitude of natural phenomena such as the stability of liquid jets (e.g., kitchen faucets of garden hoses) [1], the beading of liquids on natural (e.g., spider webs) and synthetic fibers [11] and perhaps even in fundamental biological processes such as morphogenesis [12(a)]. Tubular confinement of multiphase fluids is known to have important consequences for respiration and pulmonary disease [12(b)] and for transport processes occurring in a host of biological structures in animals ranging in scale from the arteries, veins, and capillaries of the circulatory system to microtubules and other structures within animal cells. Hierarchically organized vascular structures with tubular structures containing multicomponent fluids are also characteristic structural features of plants, influencing the fluid distribution within these structures [12(a)] and transport processes vital for life.

The study of capillary breakup has a long history. Savart [13] gave the first scientific report of the breakup of liquid threads in 1833, followed by Magnus [14] in 1855. Plateau [15] and his assistants performed experiments on the breakup of fluid threads, and Plateau provided the first theoretical explanation of the occurrence of this instability when the thread length is greater than its circumference. For threads of greater length, boundary undulations reduce the surface area for a fixed volume of fluid. Rayleigh [16] formulated the first theory of the dynamics of thread breakup in the absence of viscosity effects in either the thread or the surrounding fluid medium. He estimated that the wavelength of the undulatory instability along the thread should be comparable to the stability length (now known as the Rayleigh-Plateau stability length) estimated using thermodynamic reasoning by Plateau. Later, Weber generalized the theory to describe the combined effects of the viscosity of the fluid thread, density and surface tension [17] and Tomotika [18] included the effect of the matrix viscosity while excluding density effects. Lee and Flumerfelt [19] have given a unified treatment of fluid thread breakup that includes viscosity mismatch, density and inertial effects. The simpler Tomitika theory is suitable for understanding the breakup of viscous fluid threads having nearly the same density as the surrounding fluid. This situation often applies well to polymer mixtures, but the non-Newtonian rheology of high molecular mass polymers is often a complication in interpreting measurements on this technologically important class of fluids [3].

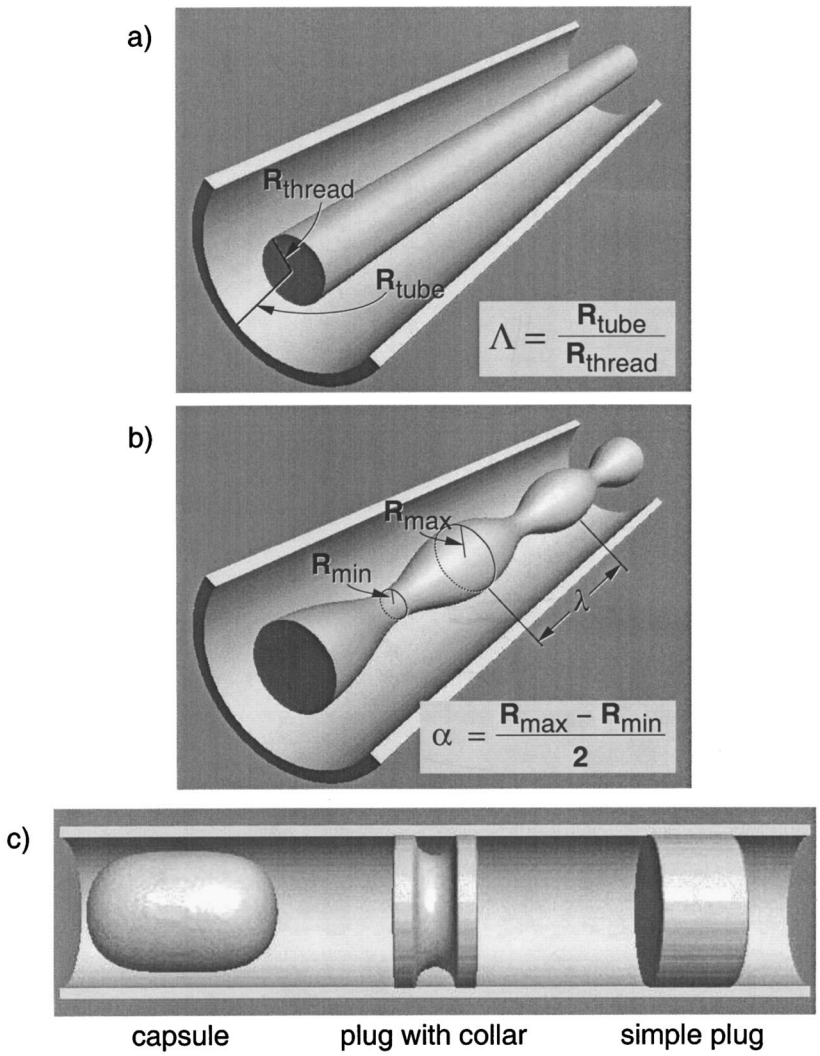

FIG. 1. Schematic illustration of thread breakup in a confining tube. (a) Initial configuration of a fluid thread confined to a tube. (b) Thread undergoing capillary undulations. The image corresponds to the simulation described below. (c) Schematic images of post-rupture structures–"plug," plug with "collar," and "capsule."

In the present paper, we are concerned about how the presence of boundaries influences the capillary breakup of viscous fluid threads and we focus particularly on the nature of thread breakup within a coaxial tube in the absence of imposed flow. Figure 1 illustrates a thread subjected to tube confinement where Fig. 1(a) shows the initial stage in which the thread has a cylindrical form, while Fig. 1(b) shows incipient thread breakup by the Rayleigh-Plateau instability [15,16]. Schematic images of the late-stage morphologies observed after thread breakup, i.e., "plugs," plugs with "collars" and "capsules" are indicated in Fig. 1(c). The collars on the plugs are transient features and these structures relax into plugs at long times. Capsules are sometimes observed to become unstable to plug formation at long times and the plugs tend to coalesce slowly at still longer times so that the late-stage evolution of the ruptured thread is characterized by a succession of long-lived transient states. Geometrical parameters that are important in specifying the simulation conditions are also indicated in Fig. 1.

Since fluid threads embedded in films (e.g., spinodal decomposition in films) and between parallel plates [20,21] are common in processing applications, we briefly compare our tube confinement simulations to those for a threads confined between two parallel plates. We also consider the breakup of arrays of threads subjected simultaneously to parallel plate confinement since multiple thread geometry illustrates some essential aspects of the influence of *flexible* boundaries on thread breakup.

In the absence of dispersion interaction effects and other non-hydrodynamic effects relevant to capillaries having a sub-micron scale [22], geometrical confinement of an infinite Newtonian thread surrounded by another liquid in a coaxial pipe does not provide thermodynamic stability against capillary breakup [9,23]. The rate of breakup and fluid morphology is certainly influenced by confinement, however [24,25]. Lubrication theory in a linearized approximation predicts that the rate of thread breakup relative to the bulk vanishes as the thread radius approaches the tube radius [23,25] and this effect has been qualitatively indicated in numerical boundary integral calculations [24]. These former simulations also indicate that the geometrical form of the thread breakup morphology changes under high confinement [24]. Notably, this type of "sharp interface" model has difficulty following the singular thread rupture and coalescence processes so that the simulations have primarily focused on phenomena occurring before thread breakup. This method also does not apply to fluids for which the interfacial width is comparable to the scale of confinement since this type of model assumes a van-

ishing interfacial width. (The interfacial width describing the composition profile or "interface" of two liquids at equilibrium can be appreciable in polymer and other complex fluids and even for "simple" fluids near thier critical point for phase separation.) We can readily treat the long time evolution of thread breakup using the lattice Boltzmann (LB) method and this allows us to obtain a more complete picture of geometric and kinetic aspects of thread breakup in confined geometries, although this method also encounters difficulties when the scale of confinement is comparable to the interfacial width (see the discussion below). The LB model is advantageous because it allows for the incorporation of polymer-fluid thermodynamic interactions that allow for surface segregation of the fluid components, a physical affect apparently difficult to incorporate in finite element and boundary element simulations of thread confinement since these models implicitly assume that the fluids are *perfectly immiscible*.

The present work focuses on the geometrical character of the thread breakup instability due to finite size effects and the influence of the fluid-surface interaction on kinetic aspects of this process using the LB model of multiphase fluid dynamics. LB simulations allow for both the treatment of a diffuse interfacial width between the liquid phases and the thermodynamic interaction between the fluid and confining wall. These interactions are commonly important in polymeric blends and other fluid mixtures (e.g., surfactant solutions) that are only weakly immiscible and the boundary interactions lead to a compositional segregation of the energetically preferred coexisting phase to the walls, thereby considerably affecting the rate of thread breakup. This effect is found in our simulations and, moreover, recent measurements have demonstrated the crucial role of fluid "wetting" properties on the stability and form of two-phase flows of immiscible fluids in microchannels [10(b)].

II. BRIEF REVIEW OF THE LATTICE BOLTZMANN MODEL AND THREAD BREAKUP IN BULK

In the LB model that we employ [27–29], the fluid within a volume element is described in terms of the particle velocity distribution function $n_a^i(x,t)$ at each point in space, $n_a^i(x,t)$ is the number of particles per unit volume at node x, time t with velocity, e_a, where the subscript $(a=1,\ldots,b)$ indicates the velocity direction and superscript i labels the fluid component. Time t evolves in discrete time steps, and the fluid particles can collide with each other as they move under applied forces. For this study, we use the D3Q19 (three dimensional lattice with $b=19$) lattice [29] where each e_a corresponds to the velocity of particles that stream to nearest neighbor sites $(1 \leqslant a \leqslant 6)$ and next nearest sites $(7 \leqslant a \leqslant 18)$ on a cubic lattice, while $e_{19}=0$ corresponds to a rest particle. The units of e_a are the lattice constant divided by the time step.

Macroscopic quantities such as the number density, $n^i(x,t)$, and the fluid velocity, u^i, of each fluid component, i, are obtained by taking suitable moment sums of $n_a^i(x,t)$. Note that while the velocity distribution function is defined only over a discrete set of velocities, the actual macroscopic velocity field of the fluid is continuous. The time evolution of the particle velocity distribution function satisfies the following LB equation:

$$n_a^i(x+e_a,t+1) - n_a^i(x,t) = \Omega_a^i(x,t), \tag{1a}$$

where the collision operator $\Omega_a^i(x,t)$ describes the rate of change of the particle distribution due to collisions. This quantity is simplified by use of the single relaxation time approximation

$$\Omega_a^i(x,t) = -\frac{1}{\tau_i}\{n_a^i(x,t) - n_a^{i(eq)}(x,t)\}, \tag{1b}$$

where $n_a^{i(eq)}(x,t)$ is the equilibrium distribution at (x,t) and τ_i controls the rate of approach to equilibrium. The equilibrium distribution can be represented in the following forms for particles of each type:

$$n_a^{i(eq)}(x) = t_a n^i(x)\left[\frac{3}{2}(1-d_o) + 3e_a\cdot u + \frac{3}{2}(3e_a e_a{:}uu - u^2)\right], \quad 1 \leqslant a \leqslant 18, \tag{2a}$$

$$n_{19}^{i(eq)}(x) = n^i(x)\left[d_o - \frac{1}{2}u^2\right] \quad (a=19), \tag{2b}$$

with $t_a=1/18$ for $1 \leqslant a \leqslant 6$ and $t_a=1/36$ for $7 \leqslant a \leqslant 18$. The number density n^i and equilibrium velocity u of the fluid mixture are then defined by the weighted averages

$$n^i = \sum_a n_a^i = \rho^i/m^i, \tag{3a}$$

$$u = \frac{\sum_i^s m^i \sum_a n_a^i e_a/\tau_i}{\sum_i^s m^i n^i(x)/\tau_i}, \tag{3b}$$

where the sum over a ranges from 1 to 19. Similarly, d_o can be related to the temperature T by the following average:

$$T(x,t) = \frac{\sum_a n_a^{i(eq)}(x,t)(e_a-u)^2}{3n^i(x,t)}. \tag{4}$$

This leads to the relation $T=(1-d_o)/2$ (units are chosen such that Boltzmann's contant equals 1). The continuum limit [27] of these LB equations leads to a velocity field that is a solution of the Navier-Stokes equation where ν is the kinematic viscosity,

$$\nu = \Delta t c^2 \frac{\sum_i^s (c_i\tau_i - 1/2)}{6},$$

with Δt the LB time step, and where c_i is the volume fraction of each ("Newtonian") fluid component.

Following Shan and Chen [27], we model fluid phase separation by introducing an interaction $[dp^i/dt(x)]$ that effectively perturbs the equilibrium velocity

$$\rho^i(x)u'(x) = \rho^i u(x) + \tau_i \frac{dp^i}{dt}(x) \tag{5}$$

u' is the new velocity used in Eq. (2). We further take the interaction to depend on the density of each fluid component:

$$\frac{dp^i}{dt}(x) = -n^i(x)\sum_{i'}^{s}\sum_{a} G^a_{ii'}\, n^{i'}(x+e_a)e_a, \tag{6}$$

with $G^a_{ii'}=2G$ for $|e_a|=1$, $G^a_{ii'}=G$ for $|e_a|=\sqrt{2}$, and $G^a_{ii'}=0$ for $i=i'$. G is a "coupling constant" that controls the strength of thermodynamic interaction between the fluids. (G is the analog of the usual "exchange or van der Waals interaction" in the usual lattice models of fluid mixtures.) It has been shown that this interaction leads to phase separation and associated critical properties (phase boundaries, correlation length, surface tension) of this model fluid mixture have recently been reported [28]. Phase separation occurs in the model upon cooling for a fixed value of G or for a critical value G_c at fixed T [28]. Comparison to measurement is facilitated by expressing G in terms of a reduced variable τ_G that ranges between 0 and 1 in the two-phase region where the fluids are immiscible, a larger value of τ_G implying a larger quench depth and interfacial tension and a smaller interfacial width between the coexisting phases [28]. In real fluids, τ_G should be taken as directly comparable to the reduced temperature $|T\text{-}T_c|/T_c$ where T_c is the critical temperature for phase separation. The LB model is notably a mean field model and does not account for fluctuation effects that can renormalize critical properties near T_c [28]. In the simulations below, we take $\tau_G=0.329$ which for a T_c near room temperature (300 K) corresponds to a quench depth of 99 K, a moderately deep quench. All distances are reported in lattice spacings or as dimensionless ratios of scales. At this quench depth, the relative volume fractions in the two coexisting phases for our model are determined to equal 0.998 and 0.002 [28].

A fluid-surface interaction is incorporated by modifying Eq. (6) in the region surrounding the fluid [28,29]. While $n^{i'}(x+e_a,t)$ normally corresponds to a particle number density, it is assigned a value 1 in Eq. (6) when $x+e_a$ resides in the solid where the value of $G^a_{ii'}$, is then set to allow the solid to attract (wet) or repulse (dewet) the fluid component i [29]. A no-slip boundary condition is maintained at the wall by utilizing a second order 'bounce back' boundary condition. Here, Eq. (1a) is replaced by $n^i_{a'}(x,t+1)-n^i_a(x,t)=\Omega^i_a(x,t)$, where a' is defined such that $e_{a'}=-e_a$.

The simulations were initialized in the following way. Denoting the two fluid components as A and B, a thread of radius R with composition $c_A=0.98$ and $c_B=0.02$ was surrounded with a fluid having composition $c_A=0.02$ and $c_B=0.98$. We then allowed the system to equilibrate. As a result, the thread radius shifted slightly. It should be appreciated that the interface between the thread liquid and the surrounding fluid is diffuse because of the moderate quench depth into the two-phase region (see Ref. [28]), creating some uncertainty about the interface position. To make its location specific, we defined the thread "boundary" as the location where the local fluid volume fraction is equal to 50%. This criterion normally corresponds to the inflection point of the composition profile governing the liquid-liquid interface [28]. We then defined the ratio of the tube radius R_{tube} to the thread radius after equilibration R_{thread} as a dimensionless measure of confinement, $\Lambda \equiv R_{\text{tube}}/R_{\text{thread}}$.

In the discussion below, we express time in terms of the rate of growth of the capillary instability in bulk, as described by the theory of Tomotika [18]. According to this theory, the amplitude $\alpha(t)$ of a perturbation of the thread boundary (infinitely long thread) grows exponentially at "early" times (see Fig. 1):

$$\alpha(t) = \alpha(0)\exp(qt), \quad t \to 0^+, \quad q = \sigma\,\Phi(\lambda,p)/2\eta_m R_{\text{thread}}. \tag{7}$$

The growth rate q depends on the interfacial tension σ, the shear viscosity η_m of the "matrix" fluid, and the viscosity of the thread η_{thr}. The "dimensionless capillary wave growth rate factor" $\Phi(\lambda,p)$ is a function of the matrix-thread viscosity ratio ($p=\eta_{thr}/\eta_m$) and wavelength λ of the perturbation and this function is tabulated by Tomotika [18] (see below). The growth rate q is maximal for the wavelength, $\lambda_{\max}=2\pi R_{\text{thread}}/\delta$, in bulk fluids (i.e., threads not subjected to confinement) where the "dimensionless wave number" δ also depends on p [18,30]. This scale grows to predominate at long times and is thus "selected" in the late stages of thread breakup. Simulation times are expressed in the reduced time, $t_{red}=q_\infty t$, where $q_\infty(R_{\text{tube}}=\infty)$ is the bulk capillary instability growth at the sclae, $\lambda_{\max}$. Confinement alters the rate of growth of the capillary instability q [or equivalently $\Phi(\lambda,p)$] and the wavelength $\lambda_{\max}$ of the disintegrating thread and theoretical and LB simulation results relating to these finite size effects are discussed below.

Our treatment of finite size effects on the rate of thread breakup is restricted to the case in which the fluid and matrix viscosities are equal ($p=1$). In this case, the Tomitika theory predicts that $\delta=0.56$ and $\Phi(\lambda_{\max},p=1)=0.0714$ [18,19]. We note for comparison that $\delta=0.69$ for the case where the viscosity of both the fluid thread and matrix are neglected ("inviscid" fluids) and that δ approaches 0 for a viscous fluid in an inviscid medium (i.e., the instability wavelength relative to the initial thread radius diverges) [16].

Our restriction to simulations of viscosity-matched fluids is made because of the large parameter space that must be investigated. Moreover, previous work on thread breakup has indicated that this assumption leads to results that are "typical" for the case where the viscosity mismatch is not large ($p\approx 1$) [24,25] and evidence for this insensitivity is described in Sec. III A.

Although no *qualitative* changes in the nature of the thread breakup should occur for modest values of viscosity mismatch, the growth rate q is affected by p and its variation is often of practical interest. Some insight into the magnitude of this effect can be obtained from tabulated values of $\Phi(\lambda_{\max},p)$ in the bulk limit [18]. While no concise analytic

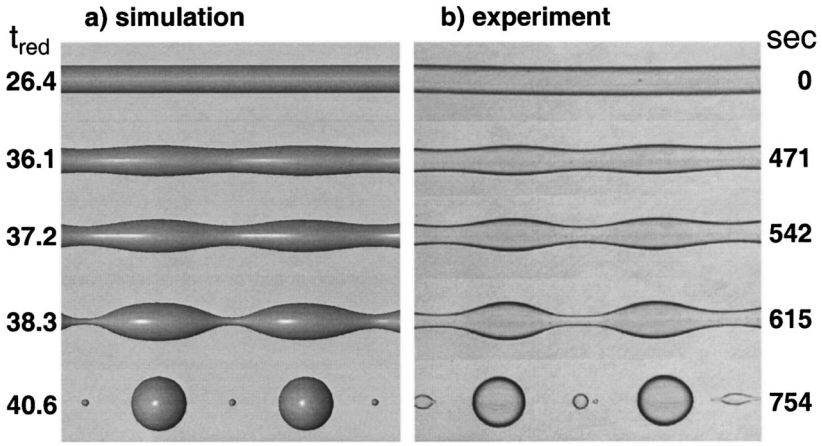

FIG. 2. Simulated and experimental fluid thread breakup under weak confinement. (a) LB simulation of a thread of radius 9.79 (in units of lattice spacing) confined to a tube of radius $24(\Lambda=2.45)$ and a length of 600. This length corresponds to about ten Rayleigh-Plateau lengths, but the image only shows a section corresponding to a couple of instability wavelengths. The time units of the simulation are given in the reduced units of thread breakup in the bulk, t_{red} (see the text). The walls of the tubes are omitted for visual clarity and to facilitate a comparison with the measurements in the accompanying figure. (b) Representative experiment of the thread breakup of a polymer thread in a polymer matrix (see the text). The time t is given in units of seconds. This measurement is for a thread confined between parallel plates and having gap to thread diameter ratio of 10.6 [21]. Confinement effects are weak in this measurement, so that these can be considered "bulk limit" observations.

expression exists for $\Phi(\lambda_{\max,p})$, even in bulk fluids, we note that $\Phi(\lambda_{\max,p})$ is reasonably well described by the Padé approximant [31]

$$\Phi(\lambda_{\max,p}) \approx (a+bp)/(1+cp+dp^2), \tag{8}$$

with $a=0.963$, $b=456.5$, $c=806.2$, and $d=12\,199$. This relation agrees with the exact results of Tomotika [18] to within a maximum deviation of 0.03 for p in the broad range between 10^{-5} to 10^{5} where $\Phi(\lambda_{\max,p})$ varies monotonically over a corresponding range between 1 and 0. From this expression we see that thread breakup generally occurs more slowly when the thread is less viscous than the matrix fluid. Simulation of thread breakup with a "large" viscosity mismatch ($p\leqslant 0.1$ or $p\geqslant 5$ requires an alternate formulation of the present LB method [32]. We defer this more general investigation to the future.

III. SIMULATION RESULTS

A. Fluid thread breakup by capillary instability under weak confinement

As a reference case and a further check of our LB mixture model of Newtonian fluid mixtures [28], we briefly consider capillary breakup of a fluid thread where finite size effects have a weak effect on the morphology of thread breakup. In Fig. 2(a), we show a progression of images of thread breakup as a function of t_{red}. The tube radius is 24 (lattice spacings) and the length of the tube (and thread) in the simulation is 600. Periodic boundary conditions are applied along the axial direction. The initial thread radius equals $R_{\mathrm{thread}}=9.9$, so that the tube length-thread aspect ratio (the length of tube L divided by R_{thread}) is approximately 60. This is about an order of magnitude larger than the Rayleigh-Plateau length $(2\pi R_{\mathrm{thread}})$ for thread breakup in bulk so that we can consider the threads as "long." In Fig. 2(a) we show only a section of the simulation (about two wavelengths) that is comparable to the measurement image for a polymer thread in a polymeric matrix shown in Fig. 2(b) (experimental conditions are summarized below). The thread was perturbed by introducing random impulsive perturbation throughout the thread, as described in Sec. III C.

The rupture of the fluid thread in Fig. 2(a) occurs through the growth of collective sinusoidal undulations about the original circular cylindrical thread, as in the schematic image shown in Fig. 1(b). At a late stage of this instability, the large amplitude regions of positive deformation (i.e., "bulges") are separated by thin, nearly circular filaments that break up by a secondary capillary instability, leading to the formation of satellite droplets [1,33–36]. A whole hierarchy of droplet sizes can be created by thread breakup through a recursive occurrence of capillary instabilities to ever-finer scales [33,35]. Treatment of these higher generations of the droplet breakup and the fine structure of the singular thread breakup morphology requires a finer discretization of the lattice model calculations. In our simulations, we observe only the leading order satellite droplets shown in Fig. 2(a). This is also often the case in measurements where various physical effects (surface tension, viscosity, non-Newtonian fluid characteristics, impurities) cut off this hierarchical instability. For example, the breakup of a polymer thread under weak confinement conditions shown in Fig. 2(b) exhibits only one well-formed "generation" of satellite droplets. (These measurements are actually performed for fluid threads under confinement between parallel plates, but the scale of confinement is so large that confinement effects are small.) We discuss these measurements further below, after further summarizing our results for the LB simulations under *weak confinement*.

We next quantify the growth rate of the capillary instability. In Fig. 3, we show a semi-log plot of the growth rate of

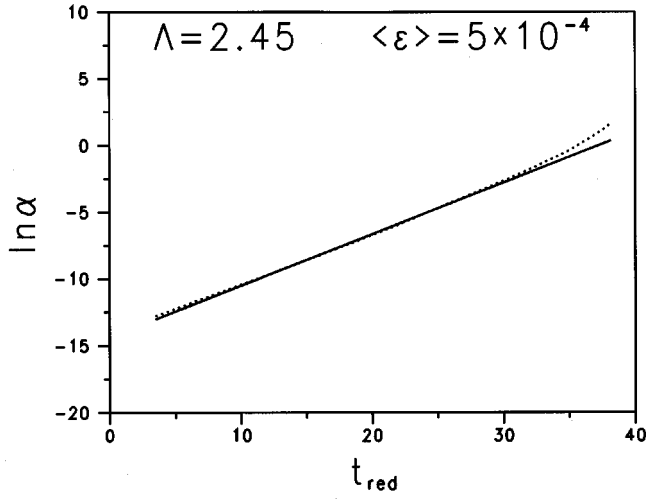

FIG. 3. Growth of capillary undulations under weak confinement conditions. α is the amplitude of the thread surface undulations and is defined as $\frac{1}{2}$ the difference between the maximum and minimum distances from the original cylindrical thread surface. Data are taken from the run shown in Fig. 2(a) and terminate at the point of thread rupture. The solid curve indicates the data range where we have fitted to the exponential growth law predicted by linearized stability theory [18], and dashed lines indicate the early "induction regime" and late stage "rupture regime" where the growth dynamics exhibits a more complicated behavior. Note the *acceleration* of the breakup process near the point of thread rupture in this example of confined thread breakup.

the thread undulation log $\alpha(t_{red})$. The nonlinear increase of log $\alpha(t_{red})$ at long times is associated with the thread rupture process and the data terminates at the time of rupture. The solid curve is a fitted "steady state" growth rate of the capillary instability and the dotted curve represents the simulation data for all times, including early and late stages where the instability growth is non-exponential. Although the size of the confining tube is sufficiently large that confinement effects do not have an appreciable influence on the *geometry* of the thread breakup process, the confinement is sufficient to influence the *rate* of thread breakup (see below). This situation is evidently similar to measuring fluid viscosity by studying the sedimentation of a sphere in a capillary [37] or the Brownian motion of a sphere in a capillary where finite size effects act over appreciable distances to affect particle mobility [38]. A typical rule of thumb is that the tube diameter should be at least an order of magnitude larger than that of the sphere diameter in order to avoid significant finite size effects [39].

The simulations described below indicate that finite size effects can substantially influence the rate of thread breakup over a large range of tube confinement and that the rule of thumb, just mentioned, describes these confinement effects reasonably well. Notably, these corrections are relevant to an accurate estimate of surface tension by observations of the dynamics of capillary breakup. Despite the potential importance of these corrections, there has been little discussion of them in the experimental literature, apart from recent work of Son *et al.* [21]. Indeed, the thread confinement scales are not normally reported [40]. Such corrections are quantified be-

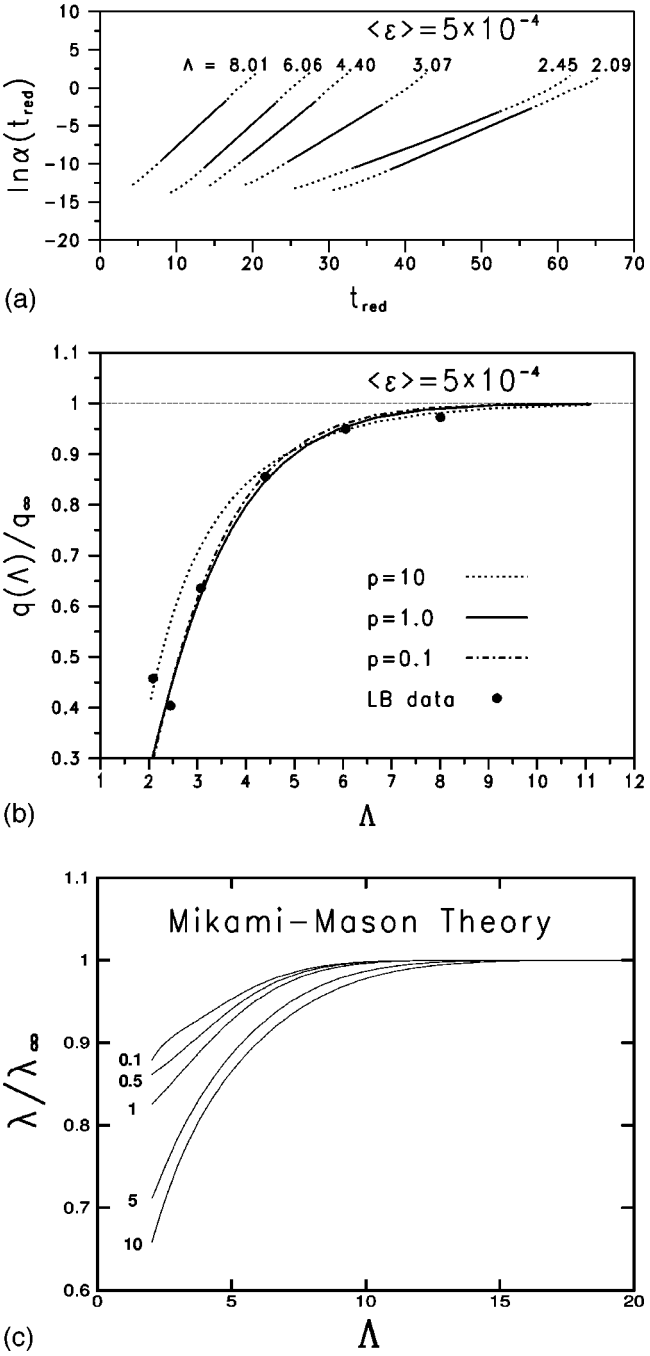

FIG. 4. Growth of capillary undulations as function of confinement, Λ. (a) The growth rate data shown in Fig. 3 is extended to the range of Λ indicated in the figure. The solid curve indicates the data range where we have fitted to the exponential growth law predicted by linearized stability theory [18], and dashed lines indicate the early "induction regime" and late stage "rupture regime" where the growth dynamics exhibits a more complicated behavior. (b) Capillary instability growth rates $q(\Lambda)$ obtained from a fit to linear portions of curves shown in (a). Growth rate data have been reduced by the bulk growth rate, $q(\Lambda \to \infty) = q_\infty$. (c) Theoretical prediction of the influence of confinement (Λ) on the wavelength $\lambda_{max}(\Lambda)$ of the maximum growth rate. Wavelength data have been reduced by the bulk value, $\lambda_{max}(\Lambda \to \infty) = \lambda_\infty$. The curves are calculated from the linearized stability theory of Mikami and Mason [41].

low for the tube geometry in the case where the matrix and thread fluids have the same viscosities and where the tube boundary does not have an energetic preference for either fluid component (see Sec. III D). Our results should be suitable for comparison with the breakup of real fluids, provided the viscosity mismatch is not too large. Equation (8) provides an estimate of the uncertainties caused by this approximation in the bulk case and we expect this expression to provide a rough estimate for the viscosity mismatch effect for the breakup of confined threads. This approximation remains to be tested, however, and should not be adopted uncritically.

In our next test of the LB model, we consider the wavelength of the most rapidly growing undulatory instability in our simulations in comparison with the analytic theory of Tomotika [18]. The dimensionless wave number δ for the data in Fig. 2(a) is equal to $\delta \approx 0.58 \pm 0.03$, where the confidence interval reflects the uncertainty in determining the λ_{max} and α due to the lattice discretization of the thread boundary. This value accords within experimental uncertainty with the theoretical value 0.56 for thread breakup in bulk (see Sec. II).

In order to quantify the role of finite size effects on the kinetics of thread breakup in the limit of "weakly confined" threads, we simulated the thread breakup for a range of Λ values between 2 and 8. The resulting growth rate data are shown in Fig. 4(a). The data from Fig. 3 ($\Lambda = 2.45$) are included for comparison in this figure. Growth rates $q(\Lambda)$ for confined threads, obtained from the linear (solid curve) portions of these curves are indicated in Fig. 4(b). (Curves have been shifted horizontally so that they do not overlap one another.) Dotted portions of curves correspond to early and late-stage regimes. Each curve in Fig. 4(a) is shifted relative to the previous curve by an amount $t_{red} = 5$, from left to right. For $\Lambda > 2.45$, the growth rate $q(\Lambda)$ increases monotonically, becoming relatively constant for $\Lambda \sim O(5-10)$. This finding accords well with the usual intuition about the scale where finite size effects tend to "saturate."

It is interesting to compare the kinetic data for thread breakup to the generalization of the Tomitika theory to confined threads derived by Mikami and Mason [41]. This theory is rather algebraically complex and does not lend itself to a closed analytic description of the rate of thread breakup, but we can accurately fit the results of this theory to analytic approximants that are useful in comparisons to our simulation data and experiment. Rigorous application of the "linearized" hydrodynamic theory is limited to "short" times, but experience has shown that this type of approximation can be a remarkably good at longer times approaching the thread rupture time and we next compare our calculations to these predictions. Figure 4(b) shows estimates of the reduced breakup rate $q(\Lambda)/q(\Lambda \to \infty)$ determined numerically from the analytic results of Mikami and Mason [41] for the cases where the viscosity of the thread η_{thr} is ten times that of the matrix fluid (dotted line), equal to that of the matrix fluid η_m (solid line) and a factor of 0.1 times η_m (dot-dashed line). By utilizing the equation discovery algorithm of Judith Devaney a NIST [41], we find that the *exact* numerical values of $q(\Lambda)/q_\infty$ determined from the Mikami-Mason theory can be described by a simple exponential function of Λ over a broad confinement range $(2.3 < \Lambda < \infty)$, i.e., $q(\Lambda, p=1)/q_\infty \approx 1 - Q \exp[-\upsilon\Lambda]$ where $q_\infty \equiv q(\Lambda \to \infty)$, $\upsilon = 0.637$, and $Q = 2.67$. The magnitude of the deviation between this approximant and the exact numerical data is generally less than 0.005 so that we do not discriminate between the approximant and the exact numerical data in Fig. 4(b). We also observe that this simple analytic expression agrees well with our LB data for $q(\Lambda, p=1)/q_\infty$, indicated by the filled circles in this figure. Notably, the value of the "bulk" capillary growth rate (q_∞) derived from this fit is used to define the time scales of our simulations below.

We also observe from Fig. 4(b) that order of magnitude changes in the ratio of the thread to matrix fluid viscosity p have a relatively small effect on the calculated $q(\Lambda)/q_\infty$ when p is small. The deviation becomes substantial, however, for large p and the upper (dotted) curve shows this effect for the representative case, $p = 10$. This relative insensitivity of $q(\Lambda)/q_\infty$ to p does not extend to other properties, such as the "wavelength of the instability," $\lambda_{max}(\Lambda)$. This point is illustrated in Fig. 4(c) which shows the analytic prediction of Mikami and Mason [41] for $\lambda_{max}(\Lambda)$, relative to its bulk value λ_∞ and for representative p values between 0.1 and 10. It is apparent that $\lambda_{max}(\Lambda)/\lambda_\infty$ depends strongly on p and the finite size dependence of this ratio becomes increasingly large as p becomes larger.

The apparent increase in $q(\Lambda)$ for $\Lambda \approx 2.1$ and the minimum near $\Lambda \approx 2.54$ in Fig. 4(b) deserves comment. Apparently, the onset of strong confinement can actually lead to an *enhancement* of the early-stage rate of capillary breakup. It must be noted, however, that the geometrical character of the thread breakup process becomes substantially modified in this confinement regime (see the detailed discussion below) so that the thread breakup process is not directly comparable to the weak confinement data ($\Lambda > 2.54$). For more confined systems ($\Lambda < 2$), we find below that thread breakup no longer occurs by a capillary instability process like that of the bulk fluid. Thus, it is not generally sensible to speak of the Rayleigh-Plateau instability under high confinement conditions. Nonetheless, we use $q(\Lambda)$ to define the dimensionless time of our simulations since the bulk measurements still provide a natural reference point for describing the relative rate thread breakup in confined threads, regardless of the mode of thread breakup. Direct comparison to measurement can be made in the same reduced time units.

We now return to the representative experimental data [21] in Fig. 2(b) for the breakup of a polymer fluid thread and compare these results to the LB simulations above. The scales of the images in Fig. 2 have been adjusted so that the initial thread sizes are comparable ($R_{thread} = 127 \mu m$). The fluid thread is a polyamide-6 (nylon) polymer and the matrix is polystyrene where the molecular masses of the polymers are relatively low to avoid significant "entanglement" effects and the temperature is rather high ($T = 503$ K) to avoid non-Newtonian effects arising from the glass transition. We also note the viscosities of the nylon and polystyrene are 300 and 1200 Pa s, respectively, so that the viscosities are not exactly matched, as they are in the simulations. Confinement effects are weak in these measurements since the thread is confined between two parallel plates where the ratio of the gap width

between the plates and the thread diameter equals 10.6. (Measurement details are given by Son *et al.* [21] and similar observations for non-polymeric fluids are described by Mason and co-workers [30].) It is apparent from Fig. 2 that the LB simulation captures the geometrical form of the "bulk" thread breakup process rather well, including the process of satellite formation.

B. Confined fluid thread breakup: Localized impulsive perturbations

In the preparation of fluid threads for observation of their breakup, it is common to subject the threads to intentional local perturbations that can influence subsequent thread breakup [30]. These perturbations are distinct from perturbations of the thread arising from equilibrium interface fluctuations associated with the thermal energy of the fluid and can have a very large impact on the time scale of the thread breakup. Alternatively, there are instances under processing conditions where we wish to stimulate thread breakup through the application of some localized external perturbation such as an acoustic or other (electric, magnetic depending on the nature and responsiveness of the fluid) field, mechanical force or laser pulse to a particular part of the fluid thread. We thus consider the influence of finite size effects on thread breakup in the case where the thread has been subjected to a localized impulsive perturbation ("tap"). Specifically, a localized impulse is directed towards the center of the thread for the duration of ten LB time steps was applied over five consecutive lattice spaces along the thread surface and parallel to the thread orientation. The magnitude of the impulse was quantified by ε, the extent of thread deformation induced at the time of its application relative to R_{thread}. Figure 5(a) illustrates the progressive breakup of a liquid thread having an initial radius of 9.47 (lattice units) and confined within a tube of radius 19 so that $\Lambda = R_{\text{tube}}/R_{\text{thread}}$ is equal to 1.9. The length of the tube is 600, again as in Fig. 2(a), but in this case we show the entire tube. The arrow in figure indicates the position where the localized impulsive perturbation was applied and the magnitude of the impulsive perturbation equals, $\varepsilon = 0.1$, which is a typical value for measurements on threads subjected to large and localized "taps" (e.g., ε in the range 0.05–0.6 are investigated in [3]). This figure indicates the full progression of the thread breakup process and new features evidently arise because of confinement. The response of the thread to "tapping" is nearly sinusoidal and rotationally symmetric about the fluid thread with a wavelength $\delta \approx 0.57 \pm 0.03$ (uncertainty estimate same as described above). This is again in close accord with bulk thread breakup [11] (see Sec. II). At these later times, we observe the growth of fluid "bulges" where the wall fluid thickens at the expense of the fluid thread. At intermittent points, this thickening becomes large enough to rupture the thread to form "plugs." (This phenomenon has been observed in liquid thread breakup in highly confined fluid threads of water in an oil matrix [10].) The thread pinch-off appears to be a nucleationlike process, corresponding to essentially random points along the thread where the thread happens to grow to a scale sufficient to lead to rupture [43].

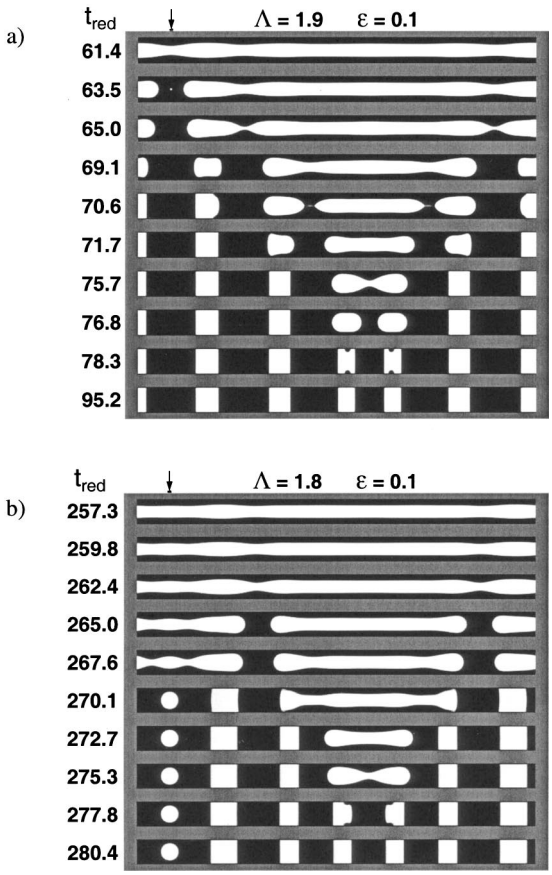

FIG. 5. Thread breakup of a strongly confined fluid threads subjected to a tapping perturbation. (a) LB simulation of a thread of radius 9.47 (in units of lattice spacing) confined to a tube of radius 18($\Lambda = 1.9$) and having a length 600. The arrow indicates the position along thread where impulsive force was applied. (b) Thread breakup evolution for a tapped thread with increased confinement ($\Lambda = 1.9$). Satellite droplets disappear by "dissolving" into the surrounding fluid. The arrow indicates the position along the thread where impulsive force was applied.

There is a correlation, however, with the rupture point and the tapping position when the tapping amplitude is sufficiently large (see. Fig. 5). The relation between the $\lambda_{\max}$ of the early-stage thread undulations to the spacing between the plugs is unclear, however. The somewhat larger distance between the plugs, relative to the initial wavelength of the instability, might give the impression of an effectively longer "instability wavelength," but this conclusion is questionable. Once the thread ruptures, we see a propagating ("end pinch") instability that grows from the ruptured thread ends towards the capsule center. A near periodic array of plugs forms as the capsule shortens through progressive fission of droplets from the capsule ends. (Propagating instabilities of this kind have also been observed in the breakup of the confined liquid capsules [10], and highly extended droplets and vesicles under flow conditions [44(a),44(b)].) Notably, satellite formation is suppressed in confined thread breakup, relative to the weak confinement case shown in Fig. 2(a). This is apparently due to the "flattening" of the thread undulation bulges of the thread due to confinement. This flattening (see Fig. 11 below where this effect is clearly illustrated for parallel plate con-

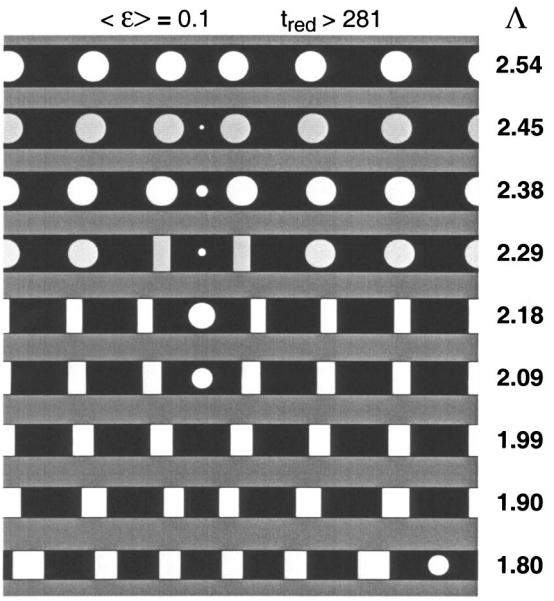

FIG. 6. Influence of tube confinement on late-stage thread breakup morphology. Image shows a cross sectional view of tube where the white fluid initially forms a cylinder at the center of tube. The initial thread radii vary from 9.44 to (in units of lattice spacing), while the tube radius varies from 17 to 25, so that Λ varies from 1.8 to 2.54.

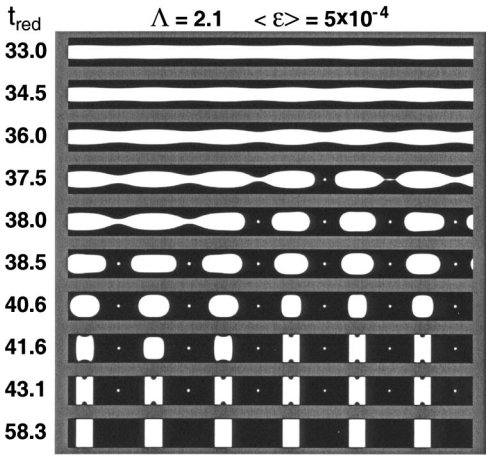

FIG. 7. Rayleigh-Plateau instability distorted by finite size effects. LB simulation of thread of initial radius 9.58 (in units of lattice spacing) confined to a tube of radius 20($\Lambda=2.09$) and having length 600. The corresponding late-stage morphology is indicated in Fig. 5.

finement) leads to a more gradual tapering of the connecting threads between the thread bulges, which then do not so readily break up into satellite droplets by capillary instability. We also find that the spacing of the plugs becomes regular in the late-stage of the capillary breakup, leading to a pattern wavelength comparable to the bulk thread breakup process. Figure 5(b) shows the case of $\Lambda=1.8$ where the confinement effect is enhanced further. It is evident that this apparently slight increase in confinement leads to a strong slowing down of the rate of thread breakup and an increase in the number of plugs.

From these observations, we conclude that morphological evolution of highly confined thread breakup is qualitatively different from unconfined or weakly confined threads ($\Lambda \geqslant 2.5$). With increasing confinement, thread breakup is predominated by non-periodic and sparse thread rupturing events. Extensive collective motion develops from these rupture points through a *propagating wave* developing along the thread which ultimately leads to a string of plugs in the tube. Once formed, the plugs are highly persistent and their coalescence is slow. This phenomenon is commonly encountered in liquid plugs formed in mercury thermometers and is appropriately named the "Jammin effect" [45].

Next, we consider the crossover between the highly confined thread breakup process in Figs. 5(a) and 5(b) and the weakly confined thread breakup process [Fig. 2(a)]. In Fig. 6, we show the late-stage morphology of the thread breakup where the tube length is fixed [see Fig. 5(a)], but Λ is varied from 1.80 to 2.54. The thread radius is near constant with small variations coming from the concentration relaxation. All the runs correspond to thread lengths well above the Rayleigh-Plateau length. The impulsive perturbation is the same as in Fig. 2(a) ($\varepsilon=0.1$). We observe a transition from plugs to droplets occurs for $\Lambda \approx 2+\theta$, where θ is on the order of the interfacial width w relative to the tube radius, w/R_{tube} where $w \approx 3$-4 lattice spacings in the present calculations. (Further measurements over a range of quench depths will be required to verify the generality of this finding.) At this scale of relative confinement, the droplets resulting from the thread breakup are just small enough to form without appreciable distortion from a spherical shape in the enclosing tube. We can appreciate the physical origin of this crossover scale by a simple geometrical argument. Assuming that the volume of the droplets formed from the ruptured thread equals the volume of a section of the thread having length $\lambda_{\max}$, implies that the radius of the droplets is equal to $R_{\mathrm{droplet}} = (3\pi/\delta)^{1/3} R_{\mathrm{thread}}$. For viscosity-matched fluids ($p=1$), this implies, $R_{\mathrm{droplet}}/R_{\mathrm{thread}} \approx 2.03$, which is close to the observed plug-droplet transition in Fig. 5. We also observe that the interdrop and interplug length scale of the late-stage pattern is not strongly sensitive to Λ. The maximum growth rate wavelength $\lambda_{\max}$ of the capillary instability at *early stages* for highly confined threads ($\Lambda \approx 1$) is predicted to equal, $\lambda_{\max} \approx 2^{3/2} \pi R_{\mathrm{thread}} (\delta = 2^{-1/2} = 0.707)$ [11]. This corresponds to a 26% *decrease* of the instability wavelength relative to breakup in the bulk matrix [18]. Although the early-stage results do not evidently apply to the morphology at long times, we note that the inter-drop spacing in the late-stage morphology is about 10% smaller than $\lambda_{\max}$ for the bulk, a trend consistent with the early-stage capillary instability theory.

A further morphological transition in the thread breakup evolution is apparent at an intermediate stage of the thread breakup for *moderate* confinement. Figure 7 shows an earlier stage evolution ($0 < t_{red} < 58.3$) of the image shown in Fig. 6 for $\Lambda=2.09$. This thread breakup process is akin to the Rayleigh-Plateau instability in bulk (Fig. 2), although the anisotropic capsules become unstable in a late-stage of the instability and form a regular array of plugs, as in the highly

confined case [Figs. 5(a) and 5(b)]. The aspect ratio of the plugs diminishes with increasing Λ, up to the plug-droplet transition range ($\Lambda = 2 + \theta$) where the droplets become nearly spherical. Note that the satellite drops "dissolve" into the surrounding fluid matrix at this moderately deep quench depth.

C. Confined fluid thread breakup: Random initial perturbation

It is known that the time of thread breakup depends on the magnitude of the initial perturbations to which the threads are subjected, although there has been limited systematic study of this phenomenon. Kuhn [46] estimated the dependence of the thread breakup time on the amplitude of random perturbations associated with *thermal fluctuations*. His estimates have not been found to agree quantitatively with measurement (presumably uncontrolled localized impulsive perturbations are one reason for this discrepancy), but they have been of value in rationalizing the existence of initial thread deformations when the data is extrapolated to $t=0$ [3,18].

The delicate interplay between thread breakup by capillary waves *all along the thread* and drops pinching off successively from the ends of capsules (end-pinch instability), described in Sec. III B, raises questions about how the thread perturbations act in connection with finite size effects. Can the *qualitative* nature of the thread breakup process depend on the character of the perturbation (e.g., discrete impulsive versus random perturbations along the thread)? To check for this possibility, we subjected the thread to small amplitude perturbations to model perturbations arising from the effect of thermal fluctuations and the thread preparation in the measurements. We find that the nature of the fluid perturbation can indeed have a strong influence on the thread breakup process in the confined regime.

A small spatially random forcing was applied at a single time step throughout the entire volume of fluid in such a way that no net momentum change occurs. The perturbation at each point was a vector of randomly determined direction, having a magnitude randomly chosen from a uniform distribution in the range $[0, 10^{-5}]$. In addition, we ensure that there is no total momentum change by pairing up lattice points of identical composition and applying a randomly generated perturbation to one member of the pair and the reverse of that perturbation to the other member of that pair. Notably, the amplitude of these random impulses is much smaller than the discrete impulses described in Sec. III B.

We first applied the random perturbations to a thread under weak confinement ($\Lambda > 2.5$). The maximum value of the scale of the impulsive deformation relative to the thread radius $\varepsilon_{\max}$ is taken to be 0.001 and the ensemble average ε is half as large, $\langle\varepsilon\rangle = 5\times10^{-4}$. These random perturbations ("kicks") were applied after the thread composition had relaxed to its coexisting composition value. For comparison, 0.001 is a typical order of magnitude for experimentally estimated values of the initial thread deformation $\alpha(t\to 0^+)$, relative to R_{thread} for threads not subjected to impulsive perturbations [3] (In measurements, these perturbation magnitudes values are normally too small for direct microscopic observation and are estimated by extrapolating the thread breakup observations to vanishing time.). We find that a change in the magnitude of $\varepsilon_{\max}$ for weakly confined threads [as in Fig. 2(a)] over a range of two orders of magnitude has little impact on asymptotic exponential growth rate of the thread breakup, apart from a change in the "induction time" it takes for the growth to approach the exponential regime [see Eq. (7) and the discussion below]. The dependence of the breakup time on the magnitude of the perturbation (ε) accords qualitatively with Kuhn's model [46], i.e., larger amplitude initial perturbations (impulsive or random) generally shorten the breakup time.

Figure 8(a) shows the influence of random perturbations in the case of a highly confined thread ($\Lambda = 1.9; \langle\varepsilon\rangle = 5\times10^{-4}$). In this case, we observe that randomness in the initial impulsive perturbation leads to a change in the early stage of thread breakup. We find that the uniform capillary undulations at short times persist to a longer time (randomness seems to stabilize the capillary instability) and the capillary undulations thus grow to a larger scale than in the "tapped" case [Fig. 5(a)]. However, the end-pinch instability ultimately intercedes to rupture the thread. Notably, the wavelength of the capillary undulations before rupture is *larger* than the bulk case by about 20%, rather than smaller, as found in the case of the "tapped" thread. The rupture of the thread is followed by an end-pinch instability that causes the formation of "peanut shaped" capsules that relax into plugs with "collars" (rings of trapped fluid within the plugs; see Fig. 1). Over time, the collars of the plugs drift to one or the other side of the plug axial face under capillary action, leaving uniformly spaced cylindrical plugs after these transient features disappear. Small plugs sometimes alternatively disappeared through a dissolution process similar to the satellite droplets described above. We also observe that the propagating (end-pinch) instability by which the thread ruptures into capsules is more rapid in the random perturbation case.

The prevalence of thread breakup by capillary instability or end-pinch instability in highly confined threads is evidently sensitive to the character of the perturbations to which the threads are subjected. Further evidence of this "noise sensitivity" in confined threads is found by increasing the confinement to $\Lambda = 1.8$ for the case of a random initial thread perturbation ($\langle\varepsilon\rangle = 5\times10^{-4}$). The breakup evolution for this case is shown in Fig. 8(b) where we find that the early-stage Rayleigh-Plateau instability, pronounced in the $\Lambda = 1.9$ case [Fig. 8(a)] is now suppressed in relation to the bulge instability and the associated end-pinch instability. Strikingly, the wavelength of the Rayleigh-Plateau instability developing at early times is *decreased* by about 10%, as in the "tapped" case [Fig. 5(a)]. This effect ultimately leads to a larger number of plugs [seven compared to six in the bulk case shown in Fig. 2(a)]. The transient capsules, formed after the thread ruptures, again develop a "peanutlike" shape and then evolve into plugs with substantial collars. In Fig. 8(b) we see that the plug collar itself ruptures in the late-stage morphology ($t_{\text{red}} \approx 579$), thus forming a droplet on the tube wall. Notably, the spacing in the plugs and the collared plug morphologies are more disordered, reflecting a sensitive dependence of the

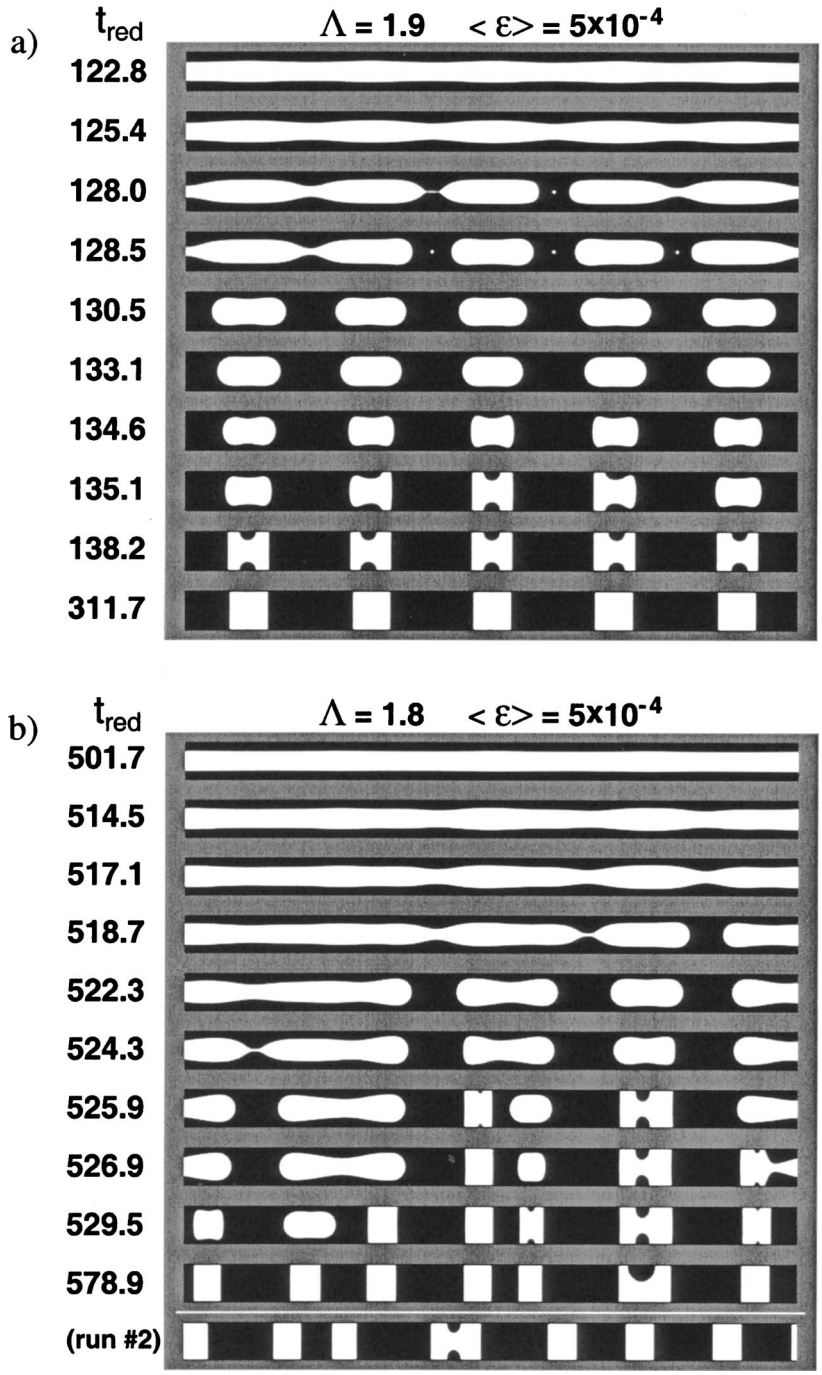

FIG. 8. Thread breakup of a strongly confined fluid threads with random perturbations. (a) LB simulation of a thread of initial radius 9.49 confined to a tube of radius 18($\Lambda = 1.9$) and having a length 600. Reduced time values t_{red} are shown in the figure. (b) Thread breakup evolution with increased confinement ($\Lambda = 1.8$).

random perturbations at earlier times. Succesive runs with different choices of random numbers describing the random thread perturbations led to distinct morphologies with similar characteristics-disorder in the plug spacings, fluctuations in the number of droplets, and odd transient "collars" on the plugs. This variation is illustrated in the last frame in Fig. 8(a) which corresponds to the morphology obtained in a second simulation at $t_{\mathrm{red}} = 578.9$. Evidently, many runs should be performed to obtain appropriately averaged properties of the thread breakup process in these highly confined fluids. These morphogical fluctuations do not occur under weak confinement conditions so that the finite size constraint amplifies the sensitivity of thread breakup to noise.

D. Confined fluid thread breakup: Influence of fluid-wall interaction

In the cases discussed so far, there is no preferential interaction between the fluid components and the capillary boundary. This interaction is found to have little effect on the breakup morphology for $\Lambda > 2.5$, but the liquid-surface interaction can be expected to be important in more confined threads. In contrast to Fig. 7, where there is no energetic preference of the thread fluid for the tube wall, Figs. 9(a) and 9(c) show the evolution in the fluid breakup ($\Lambda = 2.09$) for the cases where the fluid thread preferentially wets the tube wall and dewets the wall, respectively. Figure 9(b) indicates the energetically neutral case where neither fluid has a pref-

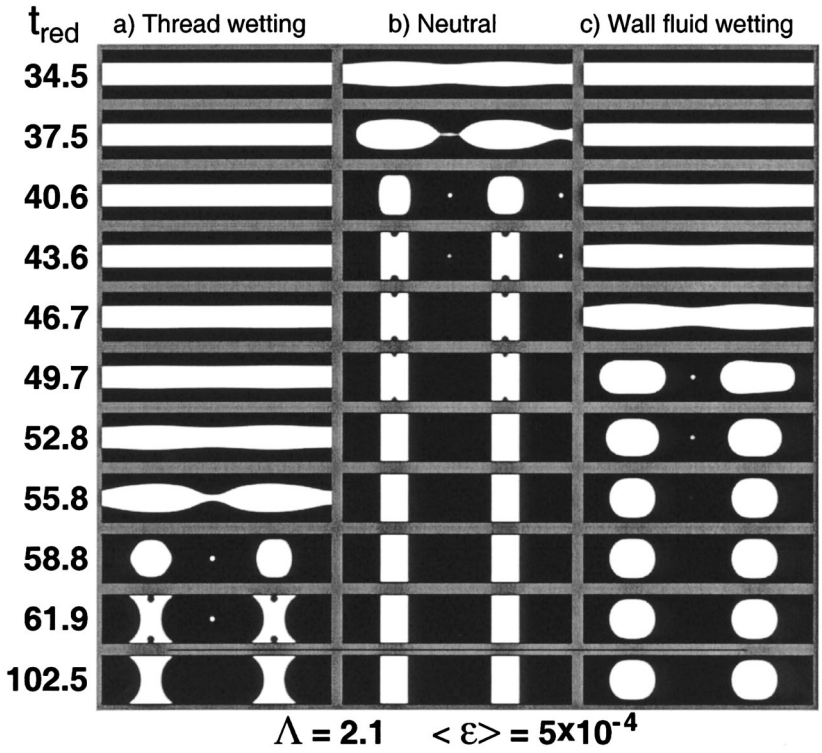

FIG. 9. Influence of surface interaction on thread breakup of confined threads. As in Fig. 7, we consider the LB simulation of thread of radius 9.55 ± 0.06 (in units of lattice spacing) that is confined to a tube of radius 20 and having length 600. (a) The thread fluid (white) preferentially wets the tube wall. (b) Fluids have the same affinity for the capillary wall. (c) The tube wall preferentially wets the annular fluid. Note that the rate of thread breakup and plug formation is slowed relative to the neutral boundary when either fluid preferentially wets the wall. These studies are performed at a fixed quench depth (interfacial width) and Λ, and future work must consider the variation of these parameters to deduce the quantitative effect of fluid-surface interaction on the rate of thread breakup.

erential affinity for the tube wall. Specifically, the equilibrium contact angles of the thread fluid on a plane surface having the interaction of the tube boundary are 35°, 90°, and 145° for Figs. 9(a)–9(c);, respectively [29]. These simulations are for the case of an impulsive thread perturbation ($\varepsilon = 0.1$), although the type of perturbation is less important for this moderate confinement case. The contact angles of the plugs directly reflect this variation in the relative energies between the fluids and the substrate. Although thread breakup occurs regardless of the relative surface energy, there is a dramatic change in the kinetics of thread breakup and plug formation arising from the fluid-tube wall interaction. First, we notice that the breakup time is greatly increased relative to the neutral wall case when *either* the thread or annular fluid has a higher affinity for the wall. In particular, the time scales t_{red} for thread rupture in Figs. 9(a)–9(c) approximately equal to 56, 38, and 50, respectively. This corresponds to about 47% and 32% increases in the thread rupture time relative to the "neutral" wall boundary condition for the case where the thread preferentially wets the surface and the wall fluid preferentially wets the surface, respectively. Unexpectedly, a high affinity of the thread fluid for the wall greatly *decelerates* the rate of thread breakup. We at first hypothesized that segregation of the tube fluid to the boundary caused a slowing of the dynamics by modifying the effective tube radius to a smaller value (thus reducing the rate of capillary breakup), but the extent of this segregation (a couple of a percent enrichment of the thread volume fraction at the wall) seems to be too small to account for the observed effect. Thus, the origin of this effect remains obscure. The stabilization of the thread rupture by the wetting of the encapsulating fluid can be more readily rationalized. The formation of plugs is clearly difficult under these circumstances and supporting this view we see that the capsules persist to long times in the simulations shown in Fig. 9(c) with this boundary interaction. (Notably we found that the capsules became plugs more rapidly in this case if the tube was made shorter, i.e., $L = 100$). These results indicate that fluid surface interactions can have a large influence on thread breakup kinetics in moderately confined geometries. This important and subtle effect will require systematic computational and experimental investigation.

E. Kinetic stabilization of thread breakup and glasslike phenomenology

Hammond [25] explained the slow growth rate of the "lobe bulging" instability of the wall fluid in the highly confined fluid regime (no thermodynamic fluid-surface interactions incorporated into the modeling) as being due to the slow rate at which the lubricating fluid surrounding the thread can "drain out" to allow the lobes to grow. A lubrication theory approximation and linearized hydrodynamic theory predicts that the rate of instability growth occurs on a time scale scaling as $(R_{\text{tube}}\eta_m/\sigma)[(R_{\text{tube}}\text{-}R_{\text{thread}})/R_{\text{tube}}]^{-3}$ where $(R_{\text{tube}}\text{-}R_{\text{thread}})/R_{\text{tube}}$ is small [see Eq. (7)]. In our units and notation, this corresponds to an instability growth rate of the confined system $q(\Lambda)$ relative to the bulk rate q_∞ which scales as $q(\Lambda)/q_\infty \sim [(\Lambda-1)/\Lambda]^3, \Lambda \approx 1$, We see that the relative value of the instability growth rate *vanishes* as the thickness of annular liquid layer vanishes. This qualitatively explains the strong effect of confinement on thread breakup kinetics under high confinement, but this result of the linearized lubrication theory is untrustworthy from a quantitative standpoint. Hammond further suggested that plug formation should be inhibited for $\Lambda \approx 1$ since at some point there should be insufficient fluid for the lobes to grow large enough to pinch off to form a plug by simple volume con-

servation. Instead, he suggested the formation of periodic lobe structures along the tube axis or "unduloid surfaces" that ultimately become separated from each other due to the pinch-off of the wall fluid at points along the tube where the layer becomes critically thin. Measurements [25,47] have not indicated the growth of such isolated fluid "collars" distributed regularly along stable fluid threads, raising questions about even the qualitative conclusions of the lubrication theory of thread breakup beyond early times. Subsequent numerical work by Gauglitz and Radke [47], based on a lubrication approximation, but with inclusion of nonlinear hydrodynamic effects relevant to describing the surface evolution at later times, indicated that thread rupture occurs beyond a "critical value of confinement," Λ^* ($\Lambda^* \approx 1.12$ for "inviscid" threads, i.e., bubbles). For Λ less than this "critical" value, the fluid thread continuity is preserved, while for greater values rupture ensues in this treatment. Measurements of the breakup of (air bubble) threads by Gauglitz and Radke [47] indicated that plug formation is largely "suppressed" for $\Lambda < \Lambda^*(\text{expt.}) = 1.09$. Moreover, thread breakup was found to be a "statistical phenomenon" in the accompanying measurements, becoming more infrequent and occurring at random along the tube for $\Lambda < \Lambda^*(\text{expt.})$. While thread breakup may occur after sufficiently long times, as suggested by the work Preziosi *et al.* [48], "effective stabilization" is obtained from a practical standpoint. Numerical studies of Newhouse and Pozrikidis [24] for *viscosity-matched* fluids ($p=1$) indicate that an arrays of lobes form below $\Lambda = 1.2$. (This estimate of the "critical confinement parameter" Λ^* is the most relevant to the present study since our fluids are likewise viscosity matched.) However, these lobes structures were found to be unstable to plug formation, which is the first stage of the end-pinch instability in our simulations. Thus, the stabilization of the threads is *not* an equilibrium phenomenon.

To gain insight into this regime of high thread confinement, we considered an additional simulation for the series shown in Fig. 5, where the tube radius was 12 and $\Lambda = 1.4$. In this case, we observe that the fluid thread remains stable up to a long time, $t_{red}=800$, consistent with the confinement-induced "stabilization" effect indicated theoretically by Hammond [26] and experimentally by Gauglitz and Radke [47]. Because of limited resolution in the lattice fluid description and the finite interfacial width arising from the relatively weak fluid immiscibilty, we performed several other simulations to see if lattice effects were influencing the apparent "stabilization" phenomenon. For example, we considered $\Lambda \approx 1.28$ for $R_{\text{tube}} = 25, 50$, and 100. It was found that for $R_{\text{tube}} = 25$ and 50, the system appeared very "stable" and we simply stopped the simulations at about $t_{red}=100$ because it did not appear to be any significant evolution of these systems, but for $R_{\text{tube}} = 100$ there was a clear indication of the onset of thread breakup after a similar time period. While it is likely that the apparent stability of these highly confined systems is affected by the lattice discretization, it should also be noted that the interfacial width becomes increasingly small relative to the thread radius in this series of simulations and this could also be a factor in the pinning phenomenon. The influence of interfacial width on thread stability will be the subject of future research.

It seems relevant at this point to note that a critical value of Λ for thread stabilization near 1.2 has been observed for fluid threads subjected to *flow* in a tube [7]. The existence of such stabilization is supported theoretically where the stabilization conditions (range of Λ for which thread stability exists depends on flow rate, viscosity ratio, etc.) [23,48], suggesting that the *kinetic stabilization* observed in the absence of flow can be converted into *absolute stability* under suitable flow conditions (see Sec. IV). The kinetic stabilization effect observed in our simulations apparently occurs over a comparable confinement range where genuine stabilization under flow occurs.

Simulation of thread stabilization by the LB method is difficult for highly confined threads ($\Lambda \leqslant 1.5$) using the current method because the interfacial width between the coexisting phases starts to become comparable to the scale of confinement (distance between tube wall and thread surface). The LB method becomes strictly *inapplicable* when the confinement scale becomes comparable to one lattice spacing, corresponding to the physical coarse graining scale of the model. (This scale is approximately the interfacial width in an infinitely deep temperature quench and can be appreciable in polymer blends and other complex fluids where the particle dimensions and the associated coarse graining scale (correlation length amplitude, ξ_o) are large [28].) To obtain further insight into the thread stabilization effect, we next consider how the time scale of thread breakup τ_B depends on Λ in a confinement regime where we are more confident in the method.

Two timescales are evident in our simulations of thread breakup, regardless of the changes in the character of the thread breakup process caused by finite size effects: (1) the time at which the fluid thread breaks τ_B, and (2) the "induction time" τ_I at which the boundary deformation $\alpha(t)$ first grows to 2% of R_{thread} so that the surface undulations are first "appreciable". This latter time is defined somewhat arbitrarily, but it does capture the notion of the onset of the thread breakup process, while τ_B characterizes its end. Figure 10 shows τ_B (solid line) and τ_I (dashed line) in reduced time units as a function of Λ for the simulations shown in Fig. 4(a) ("tapped" thread; $\varepsilon = 0.1$). The data show a sharp increase of τ_B and τ_I with decreasing Λ, but it is not clear if the divergence of these times occurs for a critical value, $\Lambda^* > 1$. The functional dependence of the increase in τ_B and τ_I is strong and, indeed, a power law in $(\Lambda\text{-}\Lambda^*)$ with a negative exponent does not seem to fit the data at all. Recognizing that this dramatic slowing down of the dynamics is due to the restricted "free volume" accessible for the displacement of the thread surface due to the confining tube, we then tried a function with an essential singularity to describe τ_B, as often employed to phenomenologically describe the strong T dependence of relaxation time data in glass-forming liquids,

$$\tau_B = A_1 \exp[E_1/(\Lambda\text{-}\Lambda^*)^2] + \tau_B{}^*, \quad A_1 = 0.663,$$

$$E_1 = 2.14, \quad \tau_B{}^* = 9.59, \tag{9}$$

where $(\Lambda\text{-}\Lambda^*)^2$ corresponds to the mean-square particle displacement in the glass-forming liquid analogy of Eq. (9) [48]. The resulting fit led to a Λ^* value close to the prediction of Newhouse and Pozrikidis [24], so we simply fix Λ^* in

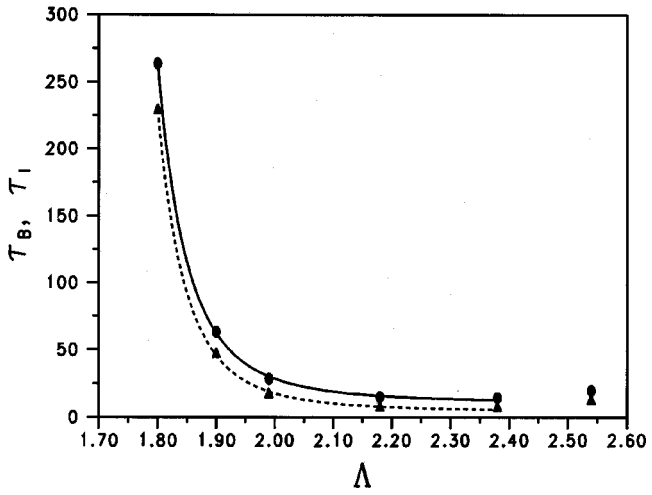

FIG. 10. Induction time τ_I and thread breakup time τ_I vs Λ. Lines are fit to Eq. (9) and (10). The solid line and the dotted line are fits to the breakup and the induction times given by Eqs. (9) and (10), respectively. The relatively small difference between these times reflects the long induction times where the thread is "thinking" about breaking up.

Eq. (9) to this value, i.e., $\Lambda^*=1.2$. Similarly, the "dimensionless induction time" τ_I data fit this same function reasonably well,

$$\tau_I = A_1 \exp[E_2/(\Lambda\text{-}\Lambda^*)^2] + \tau_I^*, \quad A_2 = 0.607,$$

$$E_2 = 2.17, \quad \tau_I^* = 6.88 \tag{10}$$

where $\Lambda^*=1.2$ and the maximum residual is 2.1. The solid line and dashed lines in Fig. 10 represent the fits to Eqs. (9) and (10), respectively. The simulation data accord with the fits to within a maximum residual of 3.2 in reduced time units for the Λ range indicated. These empirical expressions provide only a convenient parametric description that gives some sense of the rapid rate at which the dynamics of the thread breakup slows down under confinement. Note that τ_B and τ_I become fairly constant over the confinement range Λ between 2 and 2.5, despite the fact that this is still in a Λ range where finite size effects have an appreciable effect on $q(\Lambda)$ (see Fig. 4). The minimum in the data is probably a real effect associated with entering the weak confinement regime. This transition of regimes is also apparent in Fig. 4 where a substantial "kink" in the $q(\Lambda)$ data occurs near $\Lambda=2.5$. These expressions for τ_I and τ_B apply to only highly confined threads ($\Lambda<2.5$).

Although there is some quantitative uncertainty in the data regarding the lattice discretization effect described above, there is no doubt that the breakup time τ_B becomes prohibitively long to observe in both simulation and measurement with high confinement. We refer to this nonequilibrium condition as "kinetic stabilization".

F. Fluid thread breakup under confinement: Single and multiple threads between parallel plates

We now briefly consider the influence of boundary confinement on fluid threads positioned between two parallel plates, where the confining effect can be expected to be weaker than in the tube geometry. This geometry is interesting in its own right and arises in experimental studies on confined polymer blends in phase separating films [49] and immiscible polymer blends subjected to flow in a Couette apparatus where the initial droplet size is comparable to the gap spacing of the instrument [20]. Preliminary LB calculations were performed of thread breakup under parallel plate confinement to contrast this type of confinement with the tube case. These computations are briefly compared to measurements for this geometry in a separate paper where the focus was on aspects of thread breakup that are difficult to observe experimentally [21]. This subsection considers simulations for this geometry from the separate perspective of how tube confinement compares to confinement by parallel plates.

The confinement parameter Λ_{plate} for the parallel plate confinement geometry is naturally defined as the ratio of the plate gap distance H to the thread diameter. For $\Lambda_{\text{plate}} \equiv H/(2R_{\text{thread}})=1.2$, we find that the thread remains stable for a long time ($t_{red}=200$), while for $\Lambda_{\text{plate}} \geqslant 2$ the capillary breakup is not qualitatively changed from the bulk case. We show a stage of thread breakup in Fig. 11 for an intermediate value of confinement, $\Lambda_{\text{plate}}=1.43(\langle\varepsilon\rangle=5\times10^{-4})$. The side view in Fig. 11 gives a perspective of the capillary breakup process, corresponding to looking into the gap between the plates and in a direction normal to the thread orientation. The presence of the boundary attenuates the largest amplitude deformations at this stage of thread breakup as lubrication forces resist the approach of the perturbed thread surface towards the tube wall [21]. This leads to a "blunting" of the undulations on the thread into a more square-shaped waveform, an effect discussed in some detail by Son *et al.* [21]. We also observe that the thread has a nearly elliptical shape near the maximum amplitude undulations, while the thread cross-section is nearly circular in the thinned portions of the thread which are far from the tube walls [21]. A view of the thread breakup process from above the plates is shown in the top view. This is the usual experimental perspective [20,21]. Large amplitude growth regions in this projection have a more circular shape and the amplitude of these deformations is largest in regions where the lubrication forces slow the growth [21]. Finally, a profile view of the distortion in the undulating thread is shown in Fig. 11.

Comparison between the tube and parallel plate simulations indicates similarities in the thread breakup process, although evidently a greater confinement is required to achieve comparable finite size effects in the parallel plate geometry. For $\Lambda_{\text{plate}} \geqslant 2$, the breakup geometry is bulklike, while for $\Lambda_{\text{plate}}<1.2$ the process is kinetically too slow to be observable on the time scales of our simulations. For intermediate confinement (e.g., $\Lambda_{\text{plate}}=1.5$), an unstable distorted droplet ("capsule") morphology forms. These findings accord well with the measurements of Son *et al.* for polymer threads confined between parallel plates [21] and further results are briefly summarized below after discussing the LB simulations. Here we do not investigate whether a transition to nucleation thread breakup occurs for high confinement ($1.2<\Lambda_{\text{plate}}$), as in the threads in highly confined tube, because of the time consuming nature of these simulations.

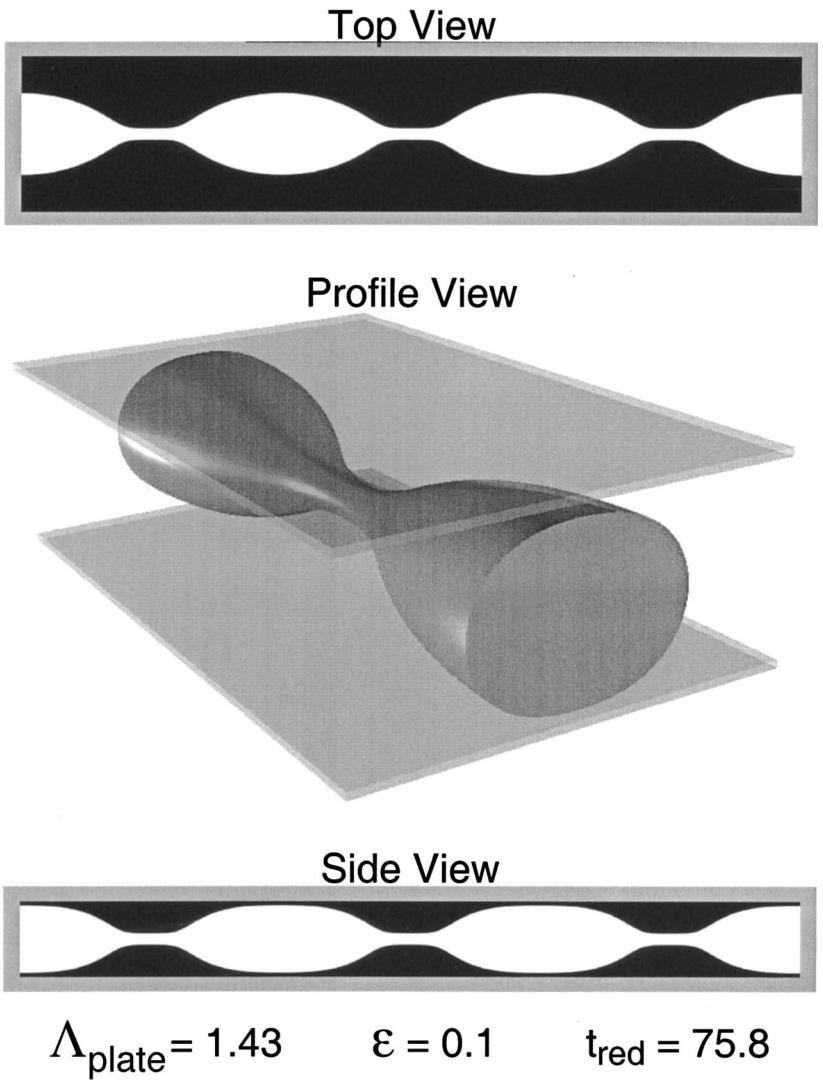

FIG. 11. Thread breakup between parallel plates under intermediate confinement conditions. LB simulation of a fluid thread having a diameter $D=106$ (in units of lattice spacing), confined between two parallel plates having a gap width $H=232$. The thread length is 600 and the width of the plates in the orthogonal direction is 480, where the boundary conditions are taken to be periodic along both these directions. The extent of confinement H/D is equal to 1.45 and $t_{red}=78.5$. Side view and end-on views at points of maximum and minimum deformation from initial cylindrical shape are shown.

However, we do anticipate a "kinetic stabilization" of the capillary instability thread breakup process and the emergence of a new mode of thread breakup at high confinement, as in the thread confined to a cylinder. Notably, the parallel plate geometry allows for the novel situation in which $\Lambda_{plate}<1$, where the cylinder must be distorted by the boundary at the outset (more of a "ribbon" than a thread). Such structures can also be considered as extended fluid plugs. Recent measurements have shown that these structures are stable under both quiescent and shear flow conditions [20]. This stability is natural given that ribbons do not break up by capillary instability in two dimensions [20,49,50].

Next, we highlight some recent measurements on thread breakup in a parallel plate geometry that are relevant to our simulations and discussion. Son *et al.* [21] find "stabilization" against thread breakup for strongly confined threads ($\Lambda_{plate}<1.3$) in the case of nylon-6 fluid threads breaking up within a confining polystyrene matrix. This finding is reminiscent of the thread breakup measurements of Gauglitz and Radke [47] for confining tubes and the simulations of threads confined to tubes. Notably, the highly confined threads of Son *et al.* [21] appeared to be stable over a time scales on the order of a day. However, these measurements indicate that finite size effects on the rate of capillary instability growth $q(\Lambda_{plate})$ are weaker than for the case of tube confinement, for the same extent of confinement. Specifically, the finite size effects apparently saturate for $\Lambda_{plate}\approx 4-5$ in the plate geometry, which a *factor of* 2 less than for the tube geometry. Based on these striking observations of thread "stabilization" under confinement, Son *et al.* [21] present a simple geometrical model of thread deformation between plates indicating that this kind of confinement leads to a *thermodynamically stable* state when Λ_{plate} is sufficiently small (i.e., $\Lambda_{plate}\leqslant 1.3$). (Notably, these arguments neglect consideration of fluid-surface interactions, which are likely relevant to determining thread stability under general circumstances.) Regardless of the exactness of this geometrical argument, there is no question that confinement leads to effective thread stabilization over very long time scales and that the thread distortion on which their argument is based actually occurs.

In summary, the "extent of confinement" $(1/\Lambda)$ must be larger in the parallel plate geometry than for the tube to achieve the same relative effect on the slowing down of the thread breakup kinetics. This trend is natural given that the tube involves confinement along two (orthogonal) directions,

while confinement occurs only along one direction in the parallel plate geometry.

We also briefly consider some aspects of thread breakup in confined geometries that arise when the confining boundary is *flexible*. Our simulations are partly motivated by our previous LB calculations [28] that showed a tendency of adjacent threads, formed under phase separation and steady flow, to undulate out of phase. (This remarkable "string phase" has been observed experimentally [51–55].) It was our impression that these collective inter-thread interactions could be crucial for understanding thread ("string") stability since isolated threads generally disintegrate under steady shear flow. We were also influenced by observations of strong inter-thread interactions in measurements modeling thread breakup in extruded polymer blends [57–60]. These fragmentary observations suggested that a "flexible" confining boundary can substantially influence thread breakup under confinement, and we thus considered a simple model to explore this effect.

Following the experiments of Elemans *et al.* [57], we consider a parallel *array of threads* confined between two parallel plates under weak confinement ($\Lambda_{\text{plate}}=2.49$) so that the *interthread interactions are the primary source of confinement*. The initial spacings between the threads was chosen to be equal to 1.7 times the thread diameter so that the inter-thread interactions are moderate. We use five threads in our simulation system and extend this computational cell periodically into the plane of confinement. Figures 12(a) and 12(b) show early and late stages of interacting thread breakup starting from random initial perturbations of the thread, where the method of applying the random perturbations and their magnitude ($\langle\varepsilon\rangle=5\times10^{-4}$) is the same as described for the tube case described in Sec. III C. First, we find that there is a long period of time occurs over which the growth of perturbations is *suppressed* by interstring interactions. (Elemans *et al.* [57] have observed a thread interaction induction time of this kind experimentally.) This long-lived, transient regime is followed by a relatively rapid thread breakup process during which the threads undulate *out of phase* with each other [Fig. 12(a)]. Once the instability starts, it develops rapidly and collectively, leading to the formation of a fairly regular droplet array [Fig. 12(b)]. Measurements of this multiple thread instability for polymer blend threads are in progress [60], but for the present we note the similarity of Fig. 12 to previous experimental observations [56]. An interesting and as yet unexplained problem is the process by which the thread undulations *phase lock* before breakup. The long induction time before thread breakup is apparently related to this phase locking phenomenon which has also been reported in the motion of microorganisms [61].

For an inter-thread spacing less than or equal to 1.5 thread diameters, the threads tended to fuse at apparently random points and subsequently formed droplets that were substantially larger than those in Fig. 12(b). This phenomenon is reminiscent of the transition to nucleated-rupture for threads subjected to high tubular confinement. Preliminary results indicate that once rupture occurs, it tends to propagate outward from its source in a wavelike fashion. This is apparently a *two-dimensional generalization of the end-pinch instability* occurring for tubular confinement. (We note that morphologically similar two-dimensional, wavelike instabilities are seen in the dewetting of thin films [62–67], suggesting another way to think about these instabilities.)

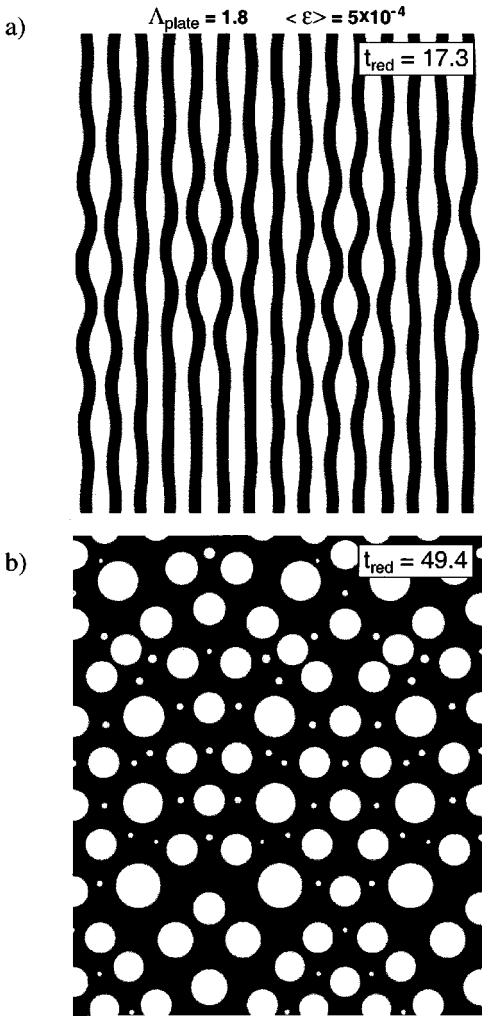

FIG. 12. Thread breakup for a thread confined between parallel plates and a periodic array of surrounding threads. The ratio of the inter-thread center spacing to the thread diameter at initial time is 1.7. The image shows a top view of plates at early stages of the thread breakup process. Simulation values of t_{red} are indicated in the figure.

IV. CONCLUSIONS

Our LB investigation indicates that confinement can substantially alter the thread breakup process from the bulk. These changes include not only changes in the rate of thread breakup, but also *qualitative* mechanistic changes in thread breakup process such as the suppression of satellite droplet formation and even the Rayleigh-Plateau instability itself. In general, the thread breakup becomes a complex admixture of capillary and end-pinch instabilities for "confined threads" ($\Lambda\leqslant1.9$) so that the nature of the thread perturbation magnitude and type (random versus impulsive "taps") can have a

large influence on the final morphology. We note that these changes in the kinetics of capillary breakup, even under weak confinement conditions (tube radius less than ten times that of thread and greater than 2.5 thread radii), have practical implications for surface tension and other property measurements based on observations of the kinetics of thread breakup in confined geometries.

A comparison between thread breakup in tube and parallel plate geometries indicate that confinement has a similar effect for both these geometries. Of course, greater confinement, as measured by $1/\Lambda$, was required to achieve the same relative effect on the slowing down of the thread breakup kinetics. This trend is natural given that the tube involves confinement along two (orthogonal) directions, while confinement occurs only along one direction in the parallel plate geometry. Our comparison also reveals some *unique characteristics* of parallel plate confinement. Specifically, the confinement parameter Λ_{plate} can be less than 1 if we allow the "threads" to deform under confinement to form fluid strips. These "ribbons" are effectively extended tubular plugs in a direction orthogonal to the plane substrate, while in the in-plane direction the boundary fluid ribbon remains free to undulate as an unconfined fluid thread. Since the Rayleigh-Plateau instability does not exist in two-dimensional systems [50], it is not surprising that these plug-like and ribbon-like aspects combine to create *highly persistent extended structures*. Such structures have been observed in the processing-relevant contexts of immiscible polymer blends subjected to a Couette flow [20] and in thin phase separating blend films [49]. Of course, this is a completely different kind of "stabilization" phenomenon than the slowing down of thread breakup due to hydrodynamic lubrication forces. Fluid-substrate thermodynamic ("wetting") interactions can be expected to have a large influence on the stabilization of both ribbon and confined thread structures and further measurements and simulations are needed to understand the interplay between geometrical and thermodynamic boundary interaction effects in these structures.

Flexible boundaries, such as those arising from surrounding fluid threads, can apparently influence thread breakup. In some cases, we find that this type of constraint leads to enhanced stability, while in other cases stability is diminished. A wide range of flexible boundary types is evidently possible (e.g., threads in supported and free-standing films, etc.) and investigation of this type of confinement is needed since many new features apparently arise for this type of confinement.

ACKNOWLEDGMENTS

We thank David Cotrell and Judith Devaney of the NIST Mathematical and Computational Sciences Division for the numerical evaluation of the reduced thread instability growth rate $q(\Lambda)/q_\infty$ from the theory of Mikami and Mason [41] and for the determination of the approximant [42] for $q(\Lambda)/q_\infty$ shown in Fig. 4(b), respectively. We also thank Jai Pathak, Steve Hudson, and Kalman Migler of the Polymers Division and Edward Garboczi and Jeffrey Bullard of the NIST Materials and Construction Research Divisions for their helpful comments on our paper. Finally, we acknowledge the NIST Center for Theoretical and Computational Materials Science for its crucial financial support at an early stage of this project.

[1] D. B. Bogy, Annu. Rev. Fluid Mech. **11**, 207 (1979).
[2] P. G. de Gennes, Rev. Mod. Phys. **57**, 827 (1985); also see Ref. [22].
[3] J. J. Elmendorp, Polym. Eng. Sci. **26**, 418 (1986); Y. Son, Polymer **42**, 1287 (2001); P. Xing, M. Bousmina, D. Rodrigue and M. R. Kamal, Macromolecules **33**, 8020 (2000). See Ref. [57] for further discussion of thread formation and breakup in extruded polymer blends and Ref. [26] regarding phase separation in tubular confined geometries.
[4] E. D. Siggia, Phys. Rev. A **20**, 595 (1979).
[5] A. V. Everage, Trans. Soc. Rheol. **17**, 629 (1973); J. H. Southern and R. L. Ballman, J. Appl. Polym. Sci. **20**, 175 (1973).
[6] T. W. F. Russel, G. W. Hodgson, and G. W. Grover, Can. J. Chem. Eng. **37**, 9 (1959); D. Hasson, U. Mann, and A. Nir, *ibid.* **48**, 514 (1970).
[7] M. E. Charles, G. W. Grover, and G. W. Hodgson, Can. J. Chem. Eng. **39**, 17 (1961).
[8] M. E. Charles and R. J. Redberger, Can. J. Chem. Eng. **40**, 70 (1961).
[9] L. Preziosi, K. Chen, and D. D. Joseph, J. Fluid Mech. **201**, 323 (1989).
[10] (a) R. W. Aul and W. L. Olbricht, J. Fluid Mech. **215**, 585 (1990); (b) R. Dreyfus, P. Tabeling, and H. Willaime, Phys. Rev. Lett. **90**, 144505 (2003); T. Thorsen, R. W. Roberts, F. H. Arnold, and S. Quake, *ibid.* **86**, 4163 (2001); A. M. Gañán-Calvo and J. M. Gordillo, *ibid.* **87**, 274501 (2001).
[11] S. L. Goren, J. Fluid Mech. **12**, 309 (1962); J. Colloid Sci. **19**, 81 (1964).
[12] (a) D'Arcy Thompson, *On Growth and Form* (Cambridge University Press, Cambridge, 1994), Chap. 3; (b) D. R. Otis, M. Johnson, T. J. Pedley, and R. D. Kamm, J. Appl. Physiol. **75**, 1323 (1993); M. Johnson, R. D. Kamm, L. W. Ho, A. Shapiro, and T. J. Pedley, J. Fluid Mech. **233**, 141 (1991).
[13] F. Savart, Ann. Chim. Phys. **53**, 337 (1833).
[14] G. Magnus, Annu. Rev. Phys. Chem. **95**, 1 (1855).
[15] J. Plateau, *Statique Experimentale et Theorique des Liquides Soumis aux Seules Forces Moleculaires* (Gaitier-Villars, Paris, 1873); Acad. Sci. Bruxelles Mém. **23**, 5 (1849).
[16] J. W. Strutt (Lord Rayleigh), Proc. R. Soc. London, Ser. A **29**, 71 (1879); Philos. Mag. **34**, 145 (1892); Also see S. Chandrasekhar, *Hydrodynamic and Hydromagnetic Stability* (Clarendon Press, Oxford, 1961).
[17] C. Weber, Z. Angew. Math. Mech. **11**, 136 (1931).
[18] S. Tomotika, Proc. R. Soc. London, Ser. A **150**, 322 (1935); also see T. Mikami, R. G. Cox, and R. G. Mason, Int. J. Multiphase Flow **2**, 113 (1975); C. M. Kinoshita, H. Teng, and S.

Masutani, *ibid.* **20**, 523 (1994); B. J. Meister and G. F. Scheele, AIChE J. **13**, 682 (1967).
[19] W.-K. Lee and R. W. Flumerfelt, Int. J. Multiphase Flow **7**, 363 (1981).
[20] K. Migler, Phys. Rev. Lett. **86**, 1023 (2001).
[21] Y. Son, N. S. Martys, J. G. Hagedorn, and K. B. Migler, Macromolecules **36**, 5825 (2003).
[22] D. Quéré, J. Di Meglio, and F. Brochard-Wyart, Science **249**, 1256 (1990).
[23] A. I. Frenkel, A. J. Babchin, B. G. Levich, T. Shlang, and G. I. Sivashinsky, J. Colloid Interface Sci. **115**, 225 (1987).
[24] L. A. Newhouse and C. Pozrikidis, J. Fluid Mech. **242**, 193 (1992). Also see J. R. Lister and H. A. Stone, J. Fluid Mech. **10**, 2758 (1998); C. Pozrikidis, J. Eng. Math. **36**, 255 (1999).
[25] P. S. Hammond, J. Fluid Mech. **137**, 363 (1983).
[26] A. J. Liu, D. J. Durian, E. Herbolzheimer, and S. A. Safran, Phys. Rev. Lett. **65**, 1897 (1990). Liu *et al.* argue that preferential fluid-wall interactions in capillaries can stabilize the coaxial thread, and capsule geometries of near-critical binary mixtures in capillaries (tubes) and discuss this phenomenon in connnection with understanding the kinetics of phase separation in porous media. In our simulations, which correspond to a fairly large quench depth, the transitions between tubes, capsules and plugs seems to be governed primarily by kinetics, where the fluid-wall interaction influences the time at which the instabilities occur. Recent molecular dynamics simulation has considered the influence of finite size effects of plug formation in phase separation [L. D. Gelb and K. E. Gubbins, Phys. Rev. E **55**, R1290 (1997)].
[27] X. Shan and H. Chen, Phys. Rev. E **47**, 1815 (1992); **49**, 2941 (1994).
[28] N. S. Martys and J. F. Douglas, Phys. Rev. E **63**, 031205 (2001).
[29] N. S. Martys and H. Chen, Phys. Rev. E **53**, 743 (1996).
[30] F. D. Rumscheidt and S. G. Mason, J. Colloid Sci. **17**, 260 (1962); H. L. Goldsmith and S. G. Mason, *ibid.* **18**, 237 (1963).
[31] This functional form for $\Phi(\lambda_{max},p)$ was fitted for us by Jai Pathak in the Polymers Division of NIST.
[32] (a) N. S. Martys, Int. J. Mod. Phys. C **12**, 1169 (2001); (b) N. S. Martys, X. Shan, and H. Chen, Phys. Rev. E **58**, 6855 (1998).
[33] M. Tjahjadi, H. A. Stone, and J. M. Ottino, J. Fluid Mech. **243**, 297 (1992).
[34] D. T. Papageorgiou, Phys. Fluids **7**, 1529 (1995).
[35] D. W. Bousfield, K. Keunings, G. Marrucci, and M. M. Denn, J. Non-Newtonian Fluid Mech. **21**, 79 (1986); also see Ref. [1].
[36] X. D. Shi, M. P. Brenner, and S. R. Nagel, Science **265**, 219 (1994).
[37] (a) J. L. Sutterby, Trans. Soc. Rheol. **17**, 559 (1973); M. Gottleib, J. Neurosci. Methods **6**, 97 (1979).
[38] H. Brenner and L. J. Gaydos, J. Colloid Interface Sci. **58**, 312 (1977).
[39] C. W. Macosko, *Rheology* (VCH, New York, 1994), p. 187.
[40] P. Xing, M. Bousmina, D. Rodrigue, and M. R. Kamal, Macromolecules **33**, 8020 (2000).
[41] Judith E. Devaney, *Lecture Notes in Computer Science*, edited by S. Arikawa and S. Morishita (Springer, New York, 2000), Vol. 167, pp. 247–251.
[42] T. Mikami and S. J. Mason, Can. J. Chem. Eng. **53**, 372 (1975).
[43] R. Xie, A. Karim, J. F. Douglas, C. C. Han, and R. A. Weiss, Phys. Rev. Lett. **81**, 1251 (1998). A reminiscent transition between capillary instability to nucleation instability is observed in the dewetting of thin liquid films.
[44] (a) H. A. Stone, B. J. Bentley, and L. G. Leal, J. Fluid Mech. **73**, 131 (1986); H. A. Stone and L. G. Leal, *ibid.* **198**, 399 (1989); H. A. Stone, Annu. Rev. Fluid Mech. **26**, 65 (1994); (b) R. Bar-Ziv and E. Moses, Phys. Rev. Lett. **73**, 1392 (1994); R. E. Goldstein, P. Nelson, T. Powers, and U. Seifert, J. Phys. II **6**, 767 (1996).
[45] D. H. Everett and J. M. Haynes, J. Colloid Interface Sci. **38**, 125 (1972).
[46] W. Kuhn, Kolloid-Z. **132**, 84 (1953).
[47] P. A. Gauglitz and C. J. Radke, Chem. Eng. Sci. **43**, 1457 (1988).
[48] L. Preziosi, K. Chen, and D. D. Joseph, J. Fluid Mech. **201**, 323 (1989); see also Ref. [10].
[49] L. Sung, A. Karim, J. F. Douglas, and C. C. Han, Phys. Rev. Lett. **76**, 4368 (1996).
[50] M. S. Miguel, M. Grant, and J. D. Gunton, Phys. Rev. A **31**, 1001 (1985).
[51] T. Hashimoto, K. Matsuzaka, E. Moses, and A. Onuki, Phys. Rev. Lett. **74**, 126 (1995).
[52] E. Moses, T. Kume, and T. Hashimoto, Phys. Rev. Lett. **72**, 2037 (1994).
[53] E. K. Hobbie, S. Kim, and C. C. Han, Phys. Rev. E **54**, 5909 (1996).
[54] S. Kim, E. K. Hobbie, and C. C. Han, Macromolecules **30**, 8245 (1997).
[55] A. H. Krall, J. V. Sengers, and K. Hamano, Phys. Rev. Lett. **69**, 1963 (1992).
[56] P. H. M. Elemans, J. M. van Wunnik, and R. A. van Dam, AIChE J. **43**, 1649 (1997).
[57] P. H. M. Elemans, J. M. H. Janssen, and H. E. H. Meijer, J. Rheol. **34**, 1311 (1990).
[58] H. E. M. Meijer, P. J. Lemstra, and J. M. H. Janssen, Makromol. Chem., Macromol. Symp. **16**, 113 (1988).
[59] Y. M.M. Knops, J. J. M. Slot, P. H. M. Elemans, and M. J.H. Bulter, AIChE J. **47**, 1740 (2001).
[60] J. A. Pathak, J. F. Douglas, N. S. Martys, J. H. Hagedorn, and K. B. Migler (unpublished).
[61] G. I. Taylor, Proc. R. Soc. London, Ser. A **209**, 447 (1951); L. J. Fauci, J. Comput. Phys. **86**, 294 (1990).
[62] O. Karthaus, L. Grasjo, N. Maruyama, and M. Shimomura, Chaos **9**, 308 (1999).
[63] R. Yerushalmi-Rosen, T. Kerle, and J. Klein, Science **285**, 1254 (1999).
[64] G. Reiter and A. Sharma, Phys. Rev. Lett. **87**, 166103 (2001); also see G. Reiter, *ibid.* **68**, 75 (1992); Langmuir **9**, 1344 (1993).
[65] C. Redon, F. Brochard-Wyart, and F. Rondolez, Phys. Rev. Lett. **66**, 715 (1991). Circular "dewetting waves" have also been observed [M. Elbaum and S. G. Lipson, *ibid.* **72**, 3562 (1994)] in evaporating water films.
[66] J. Masson, O. Olufokunbi, and P. F. Green, Macromolecules **35**, 6992 (2002).
[67] A. Vrij, Discuss. Faraday Soc. **42**, 23 (1966); F. Brochard and J. Dalliant, Can. J. Phys. **68**, 1084 (1990).